


Acknowledgement

The research project titled “Electrophoretic Deposition of *Commiphora Wightii* (Mukul), Zein, Mesoporous Bioactive Glass Nanoparticles on Titanium for Orthopedic Implants” was successfully completed in the Biomaterials Lab of the Institute of Space Technology Islamabad under the Pakistan Engineering Council (PEC) Annual Award of Final Year Design Projects (FYDPs) for the year 2022-2023. The project was supervised by Dr. Ing. Muhammad Atiq Ur Rehman.

Principal Investigator

Dr. Ing. Muhammas Atiq Ur Rehman

Assitant Professor


Assistant Professor
Materials Science & Engineering
Institute of Space Technology
(Dr. Muhammad Atiq Ur Rehman)

**ELECTROPHORETIC DEPOSITION OF *COMMIPHORA*
WIGHTII (MUKUL), ZEIN, MESOPOROUS BIOACTIVE GLASS
NANOPARTICLES ON TITANIUM FOR ORTHOPEDIC
IMPLANTS**



By

Esha Ghazanfar

Hamdaan Ahmed Quraishi

Supervisor

Dr. Muhammad Atiq Ur Rehman

Department of Materials Science and Engineering

Institute of Space Technology, Islamabad

2022

**ELECTROPHORETIC DEPOSITION OF *COMMIPHORA WIGHTII*
(MUKUL), ZEIN, MESOPOROUS BIOACTIVE GLASS
NANOPARTICLES ON TITANIUM FOR ORTHOPEDIC IMPLANTS**

A thesis submitted to the
Institute of Space Technology
in partial fulfillment of the requirements
for the degree of Bachelor of Science in
Materials Science and Engineering

By

Esha Ghazanfar

Hamdaan Ahmed Quraishi

Supervisor

Dr. Muhammad Atiq Ur Rehman

Department of Materials Science and Engineering

Institute of Space Technology, Islamabad

2022

Institute of Space Technology

Department of Materials Science and Engineering



**ELECTROPHORETIC DEPOSITION OF *COMMIPHORA WIGHTII*
(MUKUL), ZEIN, MESOPOROUS BIOACTIVE GLASS
NANOPARTICLES ON TITANIUM FOR ORTHOPEDIC
IMPLANTS**

By

Esha Ghazanfar

Hamdaan Ahmed Quraishi

APPROVAL BY BOARD OF EXAMINERS

Dr. Muhammad Atiq Ur Rehman

Internal Examiner

External Examiner

AUTHOR'S DECLARATION

We take full responsibility for the research work conducted during our BS titled, Electrophoretic deposition of *Commiphora wightii* (mukul), zein, mesoporous bioactive glass nanoparticles on titanium for orthopedic implants. We solemnly declare that the research and development work presented in our BS thesis is done solely by us with no significant help from any other person; however, small help whether taken is duly acknowledged. We have also written the complete thesis by ourselves. Moreover, we have not presented this thesis to any other degree-awarding institution within Pakistan or abroad.

We understand that the management of IST has a zero-tolerance policy towards plagiarism. Therefore, we, as the authors of the above-mentioned thesis solemnly declare that no portion of our thesis has been plagiarized and any other material used in this thesis from other sources is properly referenced. Moreover, the thesis does not contain any literal citing (verbatim) of more than 70 words (total) even by giving a reference unless we have obtained the written permission of the publisher to do so. Furthermore, the work presented in the thesis is our original work and I have positively cited the related work of the other researchers by clearly differentiating our work from their relevant work.

We further understand that if we are found guilty of any form of plagiarism in our BS thesis even after our graduation, the Institute reserves the right to revoke our BS degree. Moreover, the Institute will also have the right to publish our name on its website that keeps a record of the students who plagiarized in their thesis work.

Esha Ghazanfar

BS-11 – 180301033

Hamdaan Ahmed Quraishi

BS-11 - 180301010

I hereby acknowledge that the submitted thesis is the final version and should be scrutinized for plagiarism as per IST policy.

Dr. Muhammad Atiq Ur Rehman

Dated: _____

Verified by Plagiarism Cell Officer

Dated: _____

CERTIFICATE

This is to certify that the research work describe in this thesis is the original work of author and has been carried out under my direct supervision. I have personally gone through all the data/results/materials reported in the manuscript and certify their correctness/authenticity. I further certify that the material included in this thesis is not plagiarized and has not been used in part or full in a manuscript already submitted or in the process of submission in partial/complete fulfillment of the award of any other degree from any institution. I also certify that the thesis has been prepared under my supervision according to the prescribe format and I endorse its evaluation for the award of Master of Science in Materials Science and Engineering through the official procedures of the institute

Dr. Muhammad Atiq Ur Rehman

Dated: _____

Copyright © 2022

This document is copyrighted by the author(s), the Institute of Space Technology (IST). Only author(s), IST can use, publish, or reproduce this document in any form. Under the copyright law, no part of this document can be reproduced by anyone, except copyright holders, without the permission of the author(s).

DEDICATION

Every challenging work needs dedication, resilience, as well as guidance of the elders who are very close to our heart. Our humble effort, this thesis, we would love to dedicate it to our loving Parents whose affection, encouragement and continuous support and prayers motivated us in pursuing this research. Without their support it would not have been possible to get such a success and honour. Along with our parents, we would like to proudly thank our highly respectable supervisor, our mentor, **DR. M. ATIQ UR REHMAN** for his efforts, guidance, moral support, and encouragement throughout this whole research process.

Esha Ghazanfar

Hamdaan Ahmed Quraishi

ACKNOWLEDGMENT

All praise to Allah Almighty Who bestowed us everything to accomplish this task. First of all, I must thank our Prophet Hazrat Muhammad (S. A.W) whose teachings are just like a guiding star for us in every field of life. We could never be able to complete this if we had no blessings of Allah and His Prophet (S.A.W).

Despite a lot of hard work, late hours work on weekends, failures in optimization and trying next day with another hope and amendment in protocol, this all would have not been possible without the encouragement, cooperation, and kindness of our highly respectable supervisor Dr. M. Atiq Ur Rehman, without his thoughtful encouragement this thesis would never have taken shape. We would like to express our appreciation to the Head of Department Dr. Ibrahim Qazi for his support towards our bachelor's education.

Sincere thanks to our seniors Syeda Ammara, Memoona Akhtar, Ahmad Khan and Rabia Hussain and other members of biomaterials lab for helping in developing our skills and providing us with the assistance when requested during the period of research.

Last but not the least, we would like to specially thank to our parents for their constant support, encouragement and motivation throughout the journey, our friends and roommates who made the university and hostel experience fun and memorable.

Esha Ghazanfar

Hamdaan Ahmed Quraishi

ABSTRACT

Metals are commonly used in bone implants due to their high strength and load bearing properties. However, they are susceptible to local corrosion and biofilm formation. They are also inert which means that they cannot chemically bond with the surrounding tissues. Absence of chemical bond and micro-movements may cause dislocation of implant. These issues require an implant with enhanced bioactivity, antibacterial effect, and corrosion resistance. Orthopedic industry generally utilizes titanium (Ti) based implants due to their flexibility, biocompatibility, and corrosion resistance.

In this project, we synthesized titania nanotubes (TNTs) using electrochemical anodization method over Ti substrate for cellular ingrowth and sustained release of drugs. Next, TNTs were loaded with an antibacterial natural herb *Commiphora wightii*. Herb-loaded TNTs were further coated with zein nanoparticles (NPs) and mesoporous bioactive glass nanoparticles (MBGNs) for augmented bioactivity via electrophoretic deposition (EPD).

Coatings showed uniform deposition, good adhesion with substrate, and increased corrosion resistance in simulated body fluid (SBF). The surface roughness and wettability results indicated that the coating will be good for protein adsorption and cellular intake. The antibacterial effect against gram positive and gram-negative bacteria was also exhibited by the coating. The hydroxyapatite (HA) like structure was formed in SBF immersion analysis which is a marker of the bioactivity. The results indicated that the synthesized coating is potentially suitable for bioactive, corrosion resistant, and antibacterial orthopedic implants.

TABLE OF CONTENTS

AUTHOR'S DECLARATION	iv
DEDICATION	viii
ACKNOWLEDGMENT	ix
ABSTRACT	x
TABLE OF CONTENTS	xi
LIST OF FIGURES	xiii
LIST OF TABLES	xv
LIST OF ABBREVIATIONS	xvi
1. INTRODUCTION	1
1.1. Implants	1
1.2. Physical, Chemical & Biological Requirements	2
1.3. Orthopedic Implants	5
1.4. Problems with conventional implants	6
1.5. Problem Statement and Research Purposes	7
1.6. Complex Engineering Problem	11
1.7. Aims and Objectives	12
2. LITERATURE REVIEW	13
2.1. Titanium	13
2.2. Mesoporous Bioactive Glass Nanoparticles (MBGNs)	17
2.3. Zein	18
2.4. Herb (<i>Commiphora wightii</i>)	18

2.5. Optimization of parameters	24
3. METHODOLOGY	26
3.1. Materials	26
3.2. Preparation of Titanium substrate	26
3.3. Synthesis of TNTs	29
3.4. Annealing of TNTs substrate	31
3.5. Synthesizes of mesoporous bioactive glass Nanoparticles	31
3.6. Synthesizes of Zein NPs	32
3.7. Preparation of herb	33
3.8. Suspension preparation	34
3.9. Electrophoretic deposition of Zein NPs/MBGNs/ <i>C. wightii</i> on TNTs	35
4. RESULTS & DISCUSSIONS	46
4.1. Materials Characterization	46
5. CONCLUSIONS	61
6. FUTURE PROSPECTS	62
REFERENCES	63

LIST OF FIGURES

Fig 2.1. Formation of TNTs	15
Fig 2.2. Basic Structure of Bio Glass [21]	15
Fig 2.3. SEM, TEM images of MBGNs [27]	17
Fig 2.4. Zein Structure	18
Fig 2.5. Antibacterial Compound containing Carbonyl group	19
Fig 3.1. Sample preparation	27
Fig 3.2. Electrochemical anodization setup for the synthesis of TNTs	30
Fig 3.3. Process for the synthesis of TNTs	30
Fig 3.4. Process for the synthesis of MBGNs	32
Fig 3.5. Synthesis of zein NPs	33
Fig 3.6. (A) Gum resin (B) Powder of Commiphora Wightii	34
Fig 3.7. Process for suspension preparation	35
Fig 3.8. EPD process	36
Fig 3.9. Coatings deposited at (A) At 25 V for 7 min (B) At 30 V for 7 min (C) At 35 V for 7 min (D) At 40 V for 7min (E) & (F) At 45 V for 7 min (G) At 50 V for 5 min	38
Fig 3.10. Contact angle measurement (wettability testing)	40
Fig 3.11. Pencils according to ASTM standards	41
Fig 3.12. Process for cross-cut tape test by using a cutter	42
Fig 3.13. Disks prepared for disk diffusion test	44
Fig 3.14. Bioactivity testing of synthesized coating in SBF	45
Fig 4.1. (A) SEM Image of TNTs Surface (B) Cross section of TNTs (C) EDX spectrum	46
Fig 4.2. (A) SEM Image of MBGNs (B) EDS spectrum	47
Fig 4.3. BET Graph of MBGNs	48
Fig 4.4. (A) SEM of Zein NPs (B) EDX spectrum	49

Fig 4.5. BET Graph of Zein NPs	49
Fig 4.6. Antibacterial Test (Disk Diffusion) for <i>C.wightii</i> in different concentrations against <i>S.aureus</i> & <i>E.coli</i>	50
Fig 4.7. FTIR of Zein NPs, MBGNs, and Herb	51
Fig 4.8. (A) SEM Image of coating surface (B) SEM of coating thickness (C) Elemental mapping of coating	52
Fig 4.9. FTIR of Composite Coating	53
Fig 4.10. Pencil Test Result under Optical Microscope	54
Fig 4.11. Cross hatch test (A) before adhesive tape was applied (B) after tape was applied	55
Fig 4.12. Nano Indentation graph of coating	55
Fig 4.13. Corrosion behavior of Coated and Uncoated TNTs	56
Fig 4.14. Contact Angle (Bare and Coated TNTs)	57
Fig 4.15. Contact Angle Measurement via ImageJ software	57
Fig 4.16. (A) SEM image of Surface (7 days) (B) EDX Spectrum of Bioactivity sample (7 days)	58
Fig 4.17. (A) Bioactivity Test, (B) EDX Spectrum & (C) Elemental Mapping of 14 Days sample	59
Fig 4.18. Antibacterial Test results against <i>S. aureus</i> & <i>E. coli</i>	60

LIST OF TABLES

Table 1.1. Cost Comparison of local and imported implants (SS)	9
Table 2.1. Titanium Isotopes	13
Table 2.2. BG Compositions.....	16
Table 3.1. Trial-Error Approach Parameters	37
Table 4.1. EDX Composition of TNTs (wt% and at%).....	46
Table 4.2. EDX Composition of MBGNs (wt% and at%).....	47
Table 4.3. EDX Composition of Composite Coating	52
Table 4.4. Wave Number and related Bonds, Materials	53
Table 4.5. EDX composition of 7 days sample	58
Table 4.6. EDX composition of 14 days sample	59

LIST OF ABBREVIATIONS

μL	micro liter
μm	micrometer
ASTM	American Society for Testing of Materials
at%	Atomic %
BET	Brunauer-Emmett-Teller
BG	Bio Glass
C	Carbon
<i>C. wightii</i>	<i>Commiphora wightii</i>
Ca	Calcium
Cm	centimeter
CTAB	Cetyltrimethyl Ammonium Bromide
DC	Direct Current
DI water	Deionized Water
DoE	Design of Experiment
E_{corr}	Corrosion Potential
EDX / EDS	Energy Dispersive X-ray Spectroscopy
EPD	Electrophoretic Deposition
FTIR	Fourier-transform Infrared Spectroscopy

GPa	Giga Pascal
MPa	Mega Pascal
I_{corr}	Corrosion Current
MBGNs	Mesoporous Bioactive Glass Nanoparticles
MIC	Minimum Inhibitory Concentration
mL	milliliter
mm	millimeter
mV	millivolts
mVs^{-1}	millivolts per second
nm	nanometer
NPs	Nanoparticles
O	Oxygen
OCP	Open Circuit Potential
PEEK	Polyether ether ketone
PMMA	Polymethyl methacrylate
SEM	Scanning Electron Microscopy
Si	Silicon
SS	Stainless Steel
TEOS	Tetraethyl orthosilicate
Ti	Titanium

TiO ₂	Titania
TNTs	Titania Nanotubes
wt%	Weight %
V	Voltage
sec	Seconds
min	Minutes
h	Hours
N	Newton
mN	milli Newton
rpm	Revolutions per minute
A cm ⁻²	Ampere per centimeter square

1. INTRODUCTION

1.1. Implants

An implant is an artificially designed material that is inserted into the human body to replace defected / damaged parts such as thigh bone, joints, and teeth (dental implants). The most common type of implants are dental implants. Our focus, however, is on orthopedic implants. An orthopedic implant is the type of implant that is manufactured to replace damaged or deformed joint, bone, or cartilage. It restores the function of damaged part that has been replaced.

Implants are classified mainly as temporary and permanent.

a) Temporary Implants

Temporary implants are used when there is little damage such as fracture in a bone that can be recovered. For this purpose, this type of implants includes screws, plates, and prosthesis. They are inserted at the damaged site and holds it together until the fracture heals. These types of implants must be removed after the fracture heals. In some cases, there are temporary implants that degrade after performing their function; known as biodegradable implants.

b) Permanent Implants

Permanent implants are used when there is permanent damage to the body parts that cannot be recovered over time. These parts are then replaced by implants via surgery. Permanent implants have a lifecycle of more than 7 – 10 years depending on the type of material used and how it interacts with the body. They include hip joint, shoulder joint, knee joint, thigh bone, finger joints etc. They are mostly not biodegradable as lifelong functioning is needed from them.

1.2. Physical, Chemical & Biological Requirements

To fit into the human body is not the only requirement for an implant. There are certain properties needed in it for it to function properly in the body over a long period of time. Listed below are the physical, chemical, and biological properties required by an implant to be compatible with the body.

a) Strength

One of the major and priority requirements of an implant is its strength. Too high strength will damage the nearby bones (stress shielding effect); whereas too low stress will damage the implant itself.

The calculated strength of human bone (thigh bone) is around 30 GPa. For an implant to function properly, implant material with strength near to or equivalent to this value is required. If difference between bone's strength and implant's strength is too high, the stress on bone, when load is applied, transfers to the implant. This results in the reduction in bone density, weakening the bone and causing fracture. This phenomenon is known as stress shielding effect.

b) Ductility

If an implant is too stiff, it will be difficult to make movements properly. So, with strength, ductility is an important physical property required by an implant. Required ductility is less in thigh bone implants as compared to joints such as finger joints, hip joints, knee joints and shoulder joints where movement is necessary. Ductility and strength combination will be different depending on the type of implant being used.

c) Biocompatibility

Biocompatibility means being able to function in the human body without causing any harm to it. For an implant to function in body without causing any type of harm, it needs

to be biocompatible. It should not produce toxic or immunological response when it comes in contact with human body fluids.

d) Bioactivity

Bioactivity of a material is its positive interaction with the body while coming in contact with body's fluids or bone. This includes forming bonds with the natural body without causing any harm to it. Implant needs to be bioactive since it is replacing the bone / joint and will be in contact with surrounding fluids and natural bone all the time.

e) Surface Roughness

Living tissue and body fluids come in contact with implant material through its surface. Therefore, surface profile is important. When we insert an implant in the body, we need it to form bond with the bone or living tissue. This phenomenon is known as osseointegration, where implant and bone cannot be separated without fracture. Studies have shown that rough surface of implant promotes osseointegration. So, surface roughness of an implant is favorable as compared to smooth surface.

This property profile is also useful in drug delivery applications where medicine is targeted to the specific area of body. It can be used to store the drug / medicine until it is released into the body.[1]

f) Surface Wettability

Surface wettability is the property which tells us how a material surface interacts with any liquid that comes in contact with it. Surface wettability tells us whether the surface is hydrophilic (water loving) or hydrophobic (water hating). This is based on the measurement of contact angle. Contact angle is the angle the liquid makes when it comes in contact with the material surface. Depending on the angle, we can observe whether the surface is hydrophilic or hydrophobic. A contact angle greater than 90° means the surface is hydrophobic. On the other hand, a contact angle measurement of

less than 90° indicates hydrophilicity of the surface. Threshold value of contact angle is 90° .

Surface wettability is influenced by three forces; surface tension of liquid that is coming in contact with the surface, surface tension of the solid that is interacting with the liquid, and the interfacial tension between the liquid and solid surface.

A hydrophilic surface can support cell adhesion and blood platelet activation, which in turn enhances biocompatibility. Hydrophilicity corresponds to lubrication, which allows the liquid to slide over the surface as it interacts with it. This helps us when we are inserting the implant device into the body where body fluids interact with the surface. If the implant surface is coated, the coating must have above mentioned properties as well.

Surface roughness also affects the surface wettability directly. If a surface is rough, it will be hydrophilic, and the contact angle will be less. This will also prevent the bacteria as they will rupture after coming in contact with the rough surface.

For an implant to function well in the body, it must have good surface wettability along with roughness. Porous materials are suitable for this application [2].

g) Corrosion & Wear Resistance

Corrosion plays an important role in biomedical applications such as joint replacements and implants. In this case, surface modification plays a vital role in preventing corrosion of various types of implants including stainless steel and Titanium alloys. The type of corrosion in implants is known as biocorrosion. In order to prevent failure before death of the person operated with implants, they should also have a high corrosion resistance along with other properties mentioned above. In old patients, the service needed is around 15 -20 years and in younger patients; more than 20 years. Failure of implant due to corrosion remains one of the major issues among implant failures [3].

The human body environment is highly corrosive. It is electrolytic. The body fluids consist of blood, water, sodium, chlorine, proteins, amino acids etc. These metal ions react with the metallic implant by causing anodic and cathodic reactions at the implant surface. This also varies the pH of the environment around implant, which is around 5.3 to 5.6 against the normal body pH of 7.0.

Moreover, the metallic ion release from implants also contributes to corrosion. The limit of corrosion rate is 2.5×10^{-4} mm/year. The most common forms of corrosion that may occur in an implant are uniform corrosion, intergranular corrosion, granular corrosion, and stress corrosion cracking.

To prevent corrosion, metals with good corrosion resistance are a suitable option. To further enhance the resistance, coating the metal implant with a biocompatible non-metallic material will help.

1.3. Orthopedic Implants

It is the type of implant device that is used to replace bone fractures, in areas like thigh, joints, limb (upper or lower), or cartilage.

a) Requirements

Following are the requirements for orthopedic implants.

1. Mechanical strength
2. Flexibility (Ductility)
3. Corrosion resistance
4. Wear resistance
5. Bioactivity
6. Biocompatibility
7. Surface wettability

8. Surface roughness

All these properties have been explained above in detail.

b) Types of materials used in orthopedic implants

The most common material for implants is stainless steel. It is used mostly in thigh, limb replacements. In recent times, titanium and its alloys are also being used in these areas.

Cobalt chrome alloy is being used on the surface of metal implants for bearing properties; area of use is hip joints. Polyethylene is a common plastic used in this region in modern times as well. PMMA (polymethyl methacrylate) is also used in joint replacements. PEEK (polyether ether ketone) is also used.

Biodegradable polymers like polyglycolic acid and polylactic acid are used in biodegradable implants.

Among ceramics, calcium phosphate, zirconium oxide and silica are used as coatings on orthopedic implants [4][5].

1.4. Problems with conventional implants

Conventional orthopedic implant material is stainless steel. It is most commonly used in implant applications worldwide for a long time. However, it has some major problems listed below.

a) Lack of bioactivity

Though stainless steel is biocompatible, but it does not show any response to its surroundings in the body. This makes it inactive biologically. Due to this, stainless steel can only support the bones until they recover themselves, it does not join or fuse with the bones.

b) Biofilm formation

Since stainless steel is not bioactive, it will not resist any sort of formation of bacterial film on its surface. This can be harmful in case of implant applications.

c) Corrosion

Stainless steel has some corrosion resistance, but after some time (years), being in contact with surrounding fluids, it releases metallic ions. These ions are from the metals doped into stainless steel for its mechanical properties. These metallic ions increase the risk of corrosion as they provide more cathodic and anodic reactions. Moreover, release of toxic ions such as hexavalent chromium can have cancerous effects to human body.

d) Stress shielding effect

The calculated strength of stainless steel is around 207 GPa and that of bone is around 30 GPa. This is a huge difference. When steel is implanted in the body, it takes up all the load that is applied to the body. As a result, the bone loses its density and weakens because it is not taking up any load. This increases the risk of bone fracture. The effect is known as stress shielding effect. It occurs when the implant stays in the body for too long.

All these problems lead to revisionary surgeries that makes stainless steel uneconomical despite being less expensive and widely available as a material.

1.5. Problem Statement and Research Purposes

Bone diseases, infections and tumors leads the science towards bone regeneration by bone growth factor through implantation and tissue engineering. Small bones defects may stabilize naturally but sever bone defects that could not heal naturally require artificial fixation, implants, or substitution of bones with either autologous or allogenic grafts. For this purpose, we have synthesized our implant with specialized properties. This is a process that begins with the preparation of titanium substrate and then coating it with biomaterials and then transfer of an implant in the human body for the support

to the damaged part along with renovation properties of bone. Basically, bone is composed of organic (mainly collagen) and inorganic nanomaterials (nanohydroxapatite) with an ordered structure from nanoscale to macroscale. Therefore, for bone defects repairing and fixation some proper strategies are required to regenerate damaged tissues. Polymers, ceramics, and metals are the most commonly used biomaterials used in bone grafts, regeneration of bones and in tissue engineering for temporary or permanent substitutions to heal fractures [6]. Basically, natural bone consists of collagen fibers that support its cell function and extracellular matrix with nanosized apatitic minerals. It is beneficial for synthetically made implants to contain metallic substrate and composite coatings for the supports of cell attachments, mechanical properties like bone and encapsulated support cells for osteogenic distinctness and bone renewal.

To replace autologous or allogeneic bone the bone substitute materials must consist of bioactive glasses or ceramics, biological or synthetic polymers, and their composites. Biological polymers (collagen) help cells to promote cell attachment.

Regeneration of bone by inducing regenerating tissues in defected areas depends on the various types of interactions between the cells, implants, and growth factors [7][8]. Bone tissue engineering (TE) and bone regenerative medicine are strategies that have emerged to replace diseased bone using patient-specific cells grown on mechanically supportive substrate in vitro or to enhance the native regenerative capacity of bone using engineering and pharmacological interventions. For regeneration of bone four components are required: a morphogenetic signal, responsive host cells that will respond to the signal, a carrier that can deliver the signal to specific sites and then serve as a substrate for the growth of the responsive host cells and a viable or a well-vascularized host bed. The perfect bone tissue implants should be osteoconductive, osteoinductive,

and osteogenic [9]. Osteoconductivity requires these implants to promote the attachment, survival, towards osteoblastic lineage for bone regeneration.

Among metallic implants, stainless steel is the most common material used for implant and most of these implants have been used in orthopedic applications. Other implant materials like Ceramics, Polymers etc. are also used but not as much as metallic ones. In global implants market, the use of orthopedic implants is predicted to be doubled by the year 2025.

Table 1.1. Cost Comparison of local and imported implants (SS)

Types of Implants	Imported (PKR)	Local (PKR)
AM prothesis	28000	6000
IM IL Femoral Nail	35000	5000
DCS	24000	3000
DHS	12000	3000
IM IL Tibial Nail	35000	5000
DCP Narrow	4000	700
DCP Small	4000	600
Cortical Screws	900	100
DCP Broad	8000	1000
Cancellous Screws 6.5mm	1300	250
K-Wires	465	100
Cancellous Screws 4mm	600	150
Malleable Wires	1000	200

Within Pakistan, research was carried out on about 123 patients, over a period of 2 years, in which, locally manufactured implants were operated on patients in place of imported / branded implants [10]. Results showed that with locally manufactured implants were effective in use without any major side effect. The cost of these implants is also far less as compared to imported / branded implants. The comparison can be seen in the table 1-1. The most common material used for orthopedic implants is stainless steel. However, it has some drawbacks including lack of bioactivity, biofilm formation and corrosion [11].

we will synthesize titanium nanotubes (TNTs) over titanium substrate through electrochemical anodization method which helps to create a thin, porous layer on the implant surface which increases corrosion resistance, bone-implant bonding and osteoconduction etc. TNTs synthesized over titanium substrate will modify the surface of an implant by providing sites for protein adsorption and increasing the cell-implant interaction [12]. Anodization method will be used for the preparation of TNTs because it provides us the feasibility to change the dimensions of TNTs according to the requirements of application by controlling process parameters like electrolyte, voltage, time, temperature etc. [13]–[15]. The synthesized TNTs will be characterized by means of scanning electron microscope to analyze surface morphology and structure of TNTs and x-ray diffraction for detecting crystalline phases. At the next step, we will load our TNTs with some antibacterial drug or natural herb. At the last step, we will deposit a composite film over Ti substrate to achieve controlled drug release at the required area. For this purpose, Zein nanoparticles will be used which is a natural non-toxic polymer and mesoporous bioactive glass which is bioceramic both possessing good biocompatible and biodegradable behavior. An appropriate method for coating biodegradable polymer on electrically conductive titanium substrate will be

electrophoretic deposition (EPD) due to its cost effectiveness and relatively simple apparatus operative at room temperature [16]–[18]. At the end, the sample will be analyzed again by means of SEM to view microstructures, morphology, and topography of zein coatings.

1.6. Complex Engineering Problem

Course:

Final year project

Examples of complex engineering problem:

Electrophoretic Deposition of Zein/Mesoporous Bioactive Glass Nanoparticles (MBGNs), *Commiphora wightii* (*Mukul*), on Titanium for Orthopedic Implants

Attributes of complex problems:

1. Profound knowledge of Electrophoretic deposition technology and optimization of deposition parameters.
2. Deeper understanding of required mechanical and biological properties of zein/MBGNs/herb coating.
3. In depth analysis of obtained results from various tests to investigate efficiency and effectiveness of zein/MBGNs/herb coating.
4. Benefits for the medical welfare of society since the project involves designing coatings and synthesizing materials that will be ultimately used for treating patients with bone defects.

Attributes of complex activities:

1. Utilization of diverse resources including materials extracted from natural sources i.e., zein and *Commiphora wightii*, equipment and technology for coating fabrication characterization and performance testing.
2. Resolution of problems such as increasing bioactivity and antimicrobial effect of zein/MBGNs/herb-based coating and enhanced the mechanical properties.
3. Understanding the dependency of various factors on such as optimizing EPD parameters, enhancing mechanical properties and improving cell material interaction of coating.
4. Familiarity with various fabrication processes, Characterization techniques and performance tests required for comprehensive analysis of zein/MBGNs/herb coating.

1.7. Aims and Objectives

1. To deposit uniform coatings on TNTs.
2. To design coatings for implants with enhanced bioactivity
3. To prevent bacterial film formation

2. LITERATURE REVIEW

2.1. Titanium

Titanium was discovered in 1791 by William Gregor. It got its name from the Titans, the sons of Earth goddess of Greek mythology [19].

Titanium is a grey shiny metal. Its atomic number is 22 and has mass 48 g/mol. It lies in period 4, group 4 of the periodic table and hence is a transition metal. Melting point of titanium is 1670 °C and boiling point is 3287 °C. It is solid at room temperature.

Titanium exists as 26 isotopes ranging from ^{38}Ti to ^{63}Ti . 5 of these isotopes are stable, ^{48}Ti being the most stable among them. Isotopes with their abundance are listed in table 2.1.

Table 2.1. Titanium Isotopes

Isotope	Atomic Mass	Abundance
^{46}Ti	45.953 amu	8.25 %
^{47}Ti	46.952 amu	7.44 %
^{48}Ti	47.948 amu	73.72 %
^{49}Ti	48.867 amu	5.41 %
^{50}Ti	49.945 amu	5.18 %

Comparative to stainless steel, titanium has low density (about 4.5 g/cm³). It has high strength and high corrosion resistance. Titanium forms oxides, and the ores of titanium found are also oxides with oxidation states 4 and 3 [19].

Titanium, due to its lightweight, is used as an alloying element with different metals like molybdenum, aluminum. It is mostly used in spacecraft applications because it can withstand extreme temperatures and it also lowers the weight of vehicles.

In biomedical industry, titanium is used as an implant material. Its high corrosion resistance and relatively lower density (close to that of bone) helps the situation. Moreover, titanium is used in surgical equipment manufacture because of its inertness to the body [19].

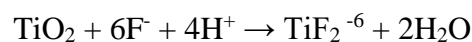
a) Titania nanotubes (TNTs)

Titania Nanotubes (TNTs) are formed by various processes. However, the preferred method is Electrochemical Anodization. TNTs have a large surface area due to the pores formed at the surface. They also have high reactivity due to this. They have photocatalytic potential and ion exchangeability.

b) Electrochemical Anodization

Anodization is a cost-effective process and requires limited equipment. It is also a time-saving technique. As a result of anodization, nanotubes are obtained at the surface of Ti substrate. The electrolyte used in this technique consists of ammonium fluoride, ethylene glycol and de-ionized water. The process takes about two hours and uniform nanotubes are obtained when voltage is set to 20 V [20]. Ti is used as a working electrode as well as counter electrode.

The process of TNTs formation occurs in three major steps. In the first step, titanium oxide layer is formed over the surface of Ti substrate. In the second stage, fluoride ions react with the TiO₂ layer to form pits on the surface. In stage 3, under application of constant voltage, the pits further form nanopores and then nanotubes with uniformity. The equation of TNTs formation is as follows.



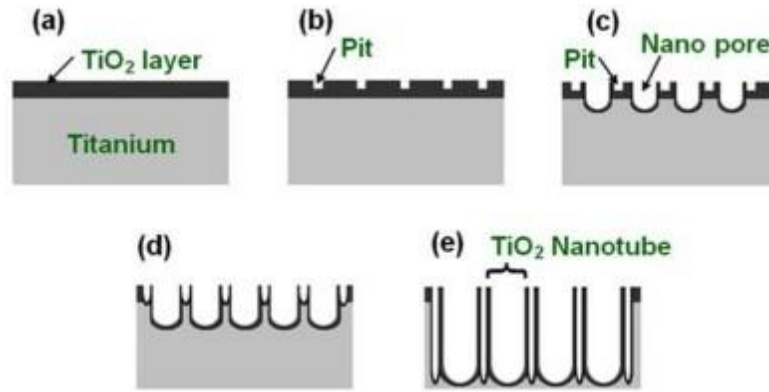


Fig 2.1. Formation of TNTs

BGs are glass-ceramics. It was first fabricated in 1969 by Larry Hench and his colleagues in Florida. The term bio glass refers to the 45S5 composition. It has osteoconductive and osteopductive properties. More compositions and properties are discussed below.

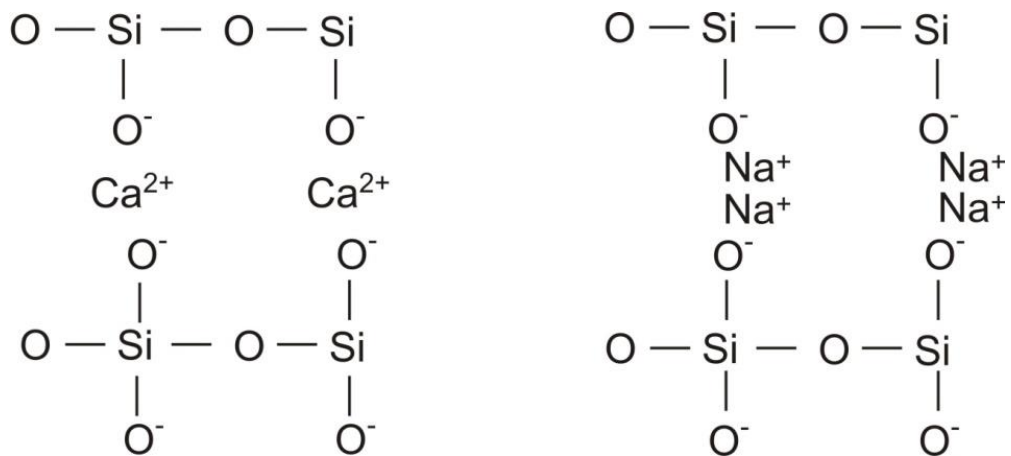


Fig 2.2. Basic Structure of Bio Glass [21]

BGs are bioactive. This is because of their high surface reactivity. This also makes them biocompatible. Their bioactivity helps them repair tissues such as bone tissues. They are used in bone repairing applications as well as tissue scaffolds and bioactive coatings. Bond formation with bone is linked to the formation of hydroxyapatite on the surface of BG. It has low fracture toughness and hence does not have good load bearing

properties. To counter this, bio glass is usually combined with polymers like PEEK etc.

This controls the stress shielding problems.

BG has various compositions based on applications. The most common type is 45S5

BG. More compositions are given in table 2.2.

Table 2.2. BG Compositions

Bio Glass	Composition	Application (soft / hard tissue repair)	Ref.
45S5	45 wt% SiO₂, 24.5 wt% CaO & Na₂O, 6 wt% P₂O₅	Hard tissue repair	[22]
S53P4	53 wt% SiO₂, 23 wt% Na₂O, 20 wt% CaO, 4 wt% P₂O₅	Hard tissue repair	[23]
58S	58 wt% SiO₂, 33 wt% CaO, 9 wt% P₂O₅	Hard tissue repair	[24]
70S30C	70 wt% SiO₂, 30 wt% CaO	Soft tissue repair	[25]
13-93	53 wt% SiO₂, 6 wt% Na₂O, 12 wt% K₂O, 5 wt% MgO, 20 wt% CaO, 4 wt% P₂O₅	Hard tissue repair	[26]

2.2. Mesoporous Bioactive Glass Nanoparticles (MBGNs)

BG has good bioactivity. To further enhance this bioactivity, mesoporous bioactive glass nanoparticles are formed. Preferred method to obtain MBGNs is stöber's process, explained below.

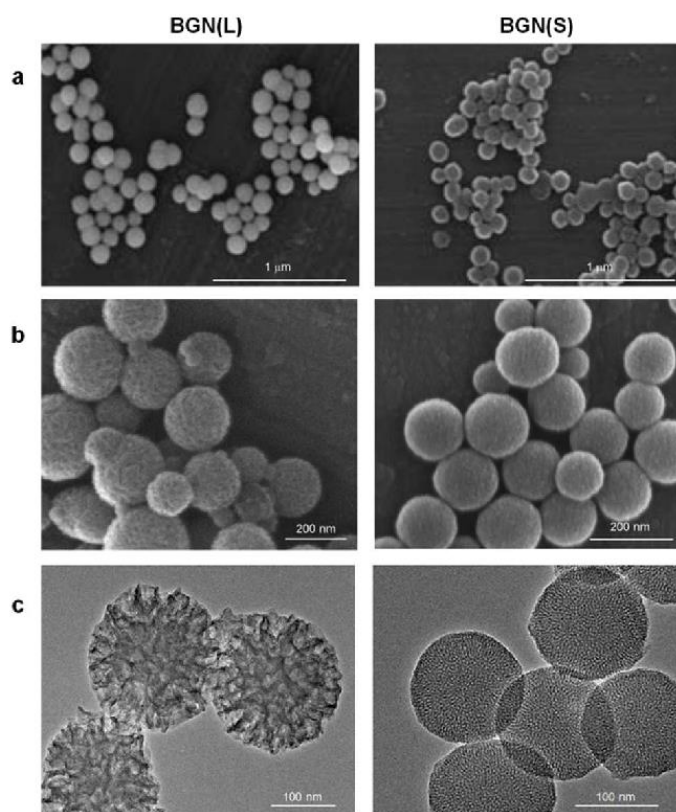


Fig 2.3. SEM, TEM images of MBGNs [27]

During the stöber process, hexadecyl trimethyl ammonium bromide (CTAB) (a surfactant) is used in the stirring solution along with ethyl acetate, distilled water, tetraethyl orthosilicate (TEOS), ammonium hydroxide and calcium nitrate. All these are added stepwise. Mesopores are formed because of CTAB which is later removed during calcination, leaving behind mesopores [28].

Mesopores formed have a pore size of 2-50 nm in diameter. This increases the surface area and hence increases bioactivity and biocompatibility. Degradation rate also

depends on pore size. The main purpose of using MBGNs is to adapt appetite-forming ability.

2.3. Zein

Zein is a biopolymer protein. It is basically corn powder and easily available from maize. It is extracted from corn. It is a type of protein and one of the best understood among plant proteins. It is biodegradable and hence, biocompatible. Zein basic structure is shown in figure 2.6.

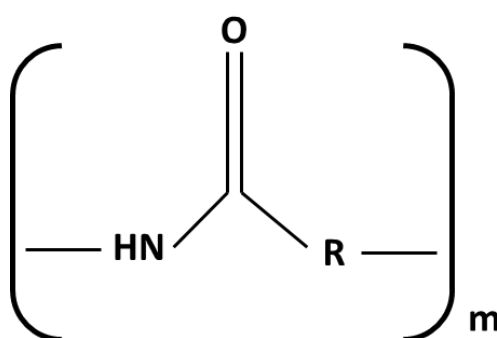


Fig 2.4. Zein Structure

Given below is the list of functional groups present in zein.

- i. Carbonyl group
- ii. Amide group
- iii. Hydroxyl group
- iv. Cyanide group [29]

2.4. Herb (*Commiphora wightii*)

Commiphora wightii is a natural herb found mostly in Southeast Asia, India. It is used by locals to treat bone diseases. It is used in the form of gum resin, roots, and leaves. The herb has osteointegrative and antibacterial properties. It can be used to bond with the bones and prevent bacterial film formation. *Commiphora wightii* has many

functional groups but the main group that gives the antibacterial effect is the carbonyl group in *commiphorine* (C₂₂H₂₂O₈).

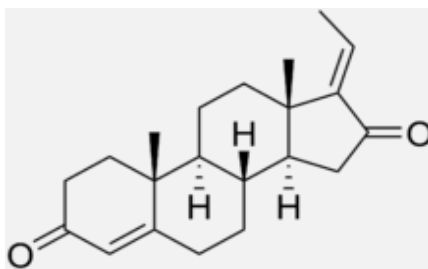


Fig 2.5. Antibacterial Compound containing Carbonyl group

Nanoscale composite coatings of biomaterials are on the interest list nowadays for biomedical applications. Complex compounds and glass/ceramics laminar particles could be easily deposited by (EPD) process [30]. EPD is a nanoscale wet deposition process which requires short time and simple apparatus for coatings. Moreover, there is no limitations of substrate shape and size, and deposition could be done on any three-dimensional (3D) substrate. By simply controlling applied voltage, time, interelectrode spacing, and suspension parameters morphology and thickness of the coatings could be adjusted. EPD process consists of a suspension containing solid particles dispersed in the solvent. When direct current (DC) is applied particles dispersed in a liquid medium get charged and migrate towards oppositely charged conductive substrate where they get deposited. The only drawback of EPD is that we cannot use water as a solvent due to chances of electrolysis. When voltage is applied, the electrolysis of water produces hydrogen and oxygen gases at electrodes which affects the quality of deposition. This problem is overcome by using non-aqueous organic solvents in the suspension [31][32].

EPD and electroplating both comes under the umbrella term of Electrodeposition. In EPD, suspension contain liquid media along with dispersed solid particles while electroplating consists of ionic solutions of salts [33]. Further, EPD is categorized into

two types; cathodic and anodic based on charged particles. If particles are positively charged, they will get deposited on cathode and the process will be called cathodic EPD, while if particles get negatively charged and deposit on anode then the process will be called anodic EPD. By modifying surface charge of particles, deposition could be possible through any mode. Hamaker describes the number of particles begin deposited on the substrate by correlating parameters affecting EPD with each other. According to Hamaker's law, deposition yield (w) of coatings could be given by:

$$w = \int_{t_1}^{t_2} \mu \cdot E \cdot A \cdot C \cdot dt$$

Where, deposition yield is directly related with electrophoretic mobility (μ), strength of electric field (E), electrode surface area (A) and mass concentration of particles in the suspension (C).

Basically, EPD process is controlled by two group of parameters to obtain homogeneous deposition [30][32].

- a) Related to the suspension
- b) Related to the process

a) Suspension related parameters

Controlling suspension related parameters is important to get a stable suspension. A stable suspension will result in the uniform deposition of particles. A coating with good mechanical stability and physio-chemical properties could be obtained with uniform deposition [32].

i. Particle size

There is no specific size range of charged particles which is suitable for EPD [31]. The only thing which is important is the complete stability and dispersion of particles in

suspension for uniform deposition. Due to gravity, larger particles tend to settle down earlier which causes difficulty to form uniform deposition. Particles form a non-uniform deposition layer and tends to accumulate at the corners of the substrate. Cracks could appear in the non- uniform deposited coatings after drying. Size reduction of particles can minimize the cracks in the deposited film [30][32].

ii. Dielectric constant of solvent

Deposition of charged particles depends on the suspension conductivity and dielectric constant of solvent. Solvents used in their pure state strongly increases the conductivity of suspension. Charged particles will only get deposited when dielectric constant of the solvent ranges within 12-25 [32][34]. When dielectric constant is too low, power dissociation occurs which fails the deposition to occur. On the other hand, when dielectric constant is very high because of high ionic concentration, it reduces the double layer formation resulting in lower electrophoresis i.e., charge mobility. Ionic concentration should remain less which is only favorable in low dielectric constant [32][35].

iii. Conduction of suspension

Conductivity of the suspension depends on the motion of the charged particles. With a little or no motion of particles, the suspension will become very conductive and if the mobility of the charged particles is very high, the suspension will become unstable [36]. There is a very narrow range of conductivity where the suspension remains stable because conductivity goes on increasing due to both the temperature and dispersed particles in the suspension. By controlling applied current, suitable range for homogeneous deposition could be obtained [32][37].

iv. Suspension viscosity

Viscosity of suspension is an important variable to be controlled. For a uniform deposition of charged particles, the viscosity should be low along with conductivity. Dielectric constant should be kept high as solid particles involved in the deposition are very less and there is no specific way that the dispersant state of the suspension could be evaluated through viscosity [32][36][37].

v. Zeta potential

In EPD process zeta potential of particles is a main factor. It is important to get highly uniform charged surface of dispersants. It also plays a key role in suspension stabilization by evaluating

- a) Repulsive forces between charged particles
- b) Direction and resettling velocity of charged particles
- c) Green density of deposition

Stability of suspension depends on the Van der Waal forces and electrostatic attraction between charged particles. The overall stability of a system depends on the interaction between individual particles in the suspension. High repulsive forces are required between charged particles to avoid coagulation. Green density of deposition also gets affected by charged particles because of attraction forces, particles come close to each other. If charge is low between particles, they get agglomerated even with large inter spacing and lead to very porous deposition while if the surface charge is high, they will repel each other and lead to the formation of deposit with high packing density of particles [38]. To get possibly highest green density it is necessary to control the concentration of solvents like acids and bases and solid particles in it. Zeta potential could be easily controlled by different charging solvents which changes the magnitude and polarity of charge [32][39].

vi. Suspension stability

Stability of suspension is evaluated based on settling and agglomeration rate of particles because stable suspensions for highly dense and adherent deposits are those who have slow settling rate with no coagulation. Too stable suspension has repulsive forces which cannot overcome by applied electric field and the deposition will not occur while suspensions with high flocculation rate will settle down rapidly and form deposits of very low density and weak adherence. Therefore, it is necessary to find suitable range of parameters where stable suspension can be obtained [32][40].

b) Process related parameters

There are some parameters which are related to the suspension but there are also some parameters which control the process to get homogenous deposition after getting stable suspension [32].

i. Deposition time

It is found that initially there is a linear relationship between the rate of deposition and time at constant voltage rate but once the potential difference becomes constant between electrodes, the impact of electric field on the electrophoretic process decreases because of deposit layer formation on the substrate [32][41][42][43].

ii. Applied potential

Deposition rate increases when applied voltage increases because the formation of deposit layer on substrate is through kinetic phenomena. Therefore, at higher applied potential charged particles move so fast that they cannot get enough time to form highly dense structure and started to get accumulated at one place because of restriction charge

particles lateral motion and high pressures on particles movement which affects the structure of deposits [32][42].

iii. Solid concentration in suspension

Deposition rate could be easily controlled by the amount of powder used in the suspension. In EPD suspension fractional volume of solid particles plays a key role specially in composite suspension. If fractional volume of particles is high, then their deposition rate would be equal but if fractional volume is less then then deposition rate of particles would be different depends on the mobility of individual species [32][44].

iv. Substrate conductivity

Along with stable and conductive suspension it is important that the substrate on which particles will get deposit should be polished, uniform, and conductive enough to complete the circuit so that electric field will be applied to the charged particles so that they get attracted towards substrate and attach to its surface in a closed pack structure for homogeneous deposition [32].

2.5. Optimization of parameters

There are two ways for the optimization of parameters.

a) Taguchi design of experiment (DoE) approach

By using Taguchi design of experiment approach, we need to find the parameters which affect the process on a great rate and the little changes in them can vary the results of experiment and had great effect on the rate of deposition. From that we can evaluate best processing conditions for the experiment while keeping other factors constant which have little or no impact on the process. Then using those optimized parameters on which uniform deposition could be obtained further used for experiment [45][46].

b) Trial error approach

This approach is also based on the idea of Taguchi DoE approach that which parameters had great effect on the rate of deposition and which parameters we need to kept constant. After that by only varying that parameters number of experiments could be done to get the best processing conditions while keeping other parameters at constant. Then from varying factors the parameters on which uniform deposition is obtained are optimized for that experiment.

3. METHODOLOGY

3.1. Materials

This research was carried out on 99% pure Ti substrate. Phenolic resin is used in mounting and alumina paste in polishing. For the synthesizes of TNTs ethylene glycol (Sigma-Aldrich), ammonium fluoride (Sigma-Aldrich) and Deionized water from local market is used [47][48][49]. After that, materials used for composite coatings on substrate are acetic acid purchased from VWR International (Shanghai, China), ethanol purchased from Sigma Aldrich (Taufkirchen, Germany), *Commiphora Wightii* purchased from local market, synthesized mesoporous bioactive glass and zein nanoparticles [50].

For the synthesis of zein nanoparticles zein powder purchased from Sigma Aldrich is used [50]. By using modified Stöber process [51] for the synthesizes of pure mesoporous bioactive glass nanoparticles with the composition of 70% SiO₂ and 30% CaO, chemicals such as 98% -hexadecyltrimethylammonium bromide (CTAB), 99%-tetraethyl orthosilicate (TEOS) were purchased from Sigma-Aldrich, and 99.5%-ethyl acetate was purchased from Merck, Darmstadt, Germany. Quantity of salts was used according to the recipe from Bano et al. [52].

3.2. Preparation of Titanium substrate

First sample preparation was done as we got commercially pure Ti substrate in the form of sheets from market which are very thin and long. As we know, this research is for biomedical purpose, and we were developing something which needs to be insert in the human body. For which substrate surface should be cleaned enough, therefore, we need to perform some operations on its surface.

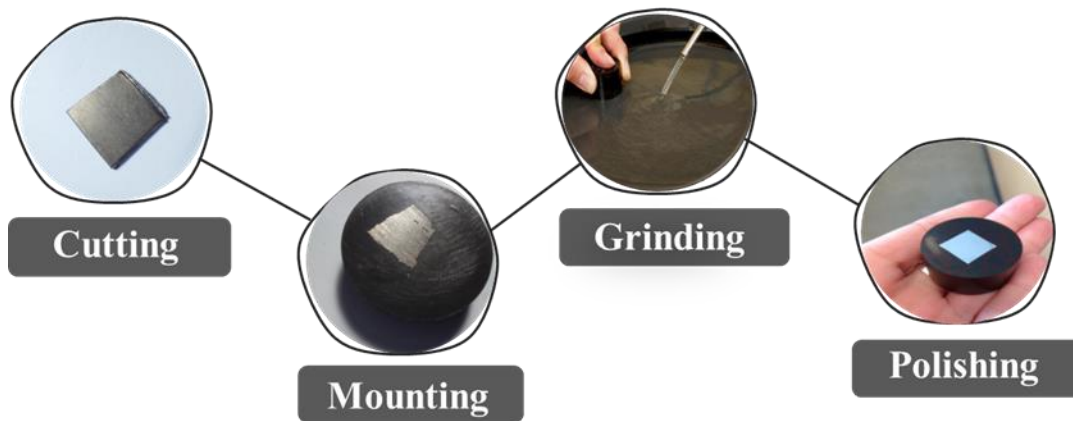


Fig 3.1. Sample preparation

First step was cutting the sheets in the form of small strips having dimensions of 2 cm \times 2 cm \times 0.1 cm by means of shear cutter purchased from local market for our ease to carry other cleaning processes. As it was difficult to grind and polish the strips manually because they were very thin. Therefore, hot mounting was performed.

a) Mounting

Sample was cleaned with DI water and ethanol and dried with blower. After that specimen was placed in a mounting cylinder in a hot mounting press (METAPRESS-M), and the appropriate mounting resin is added after placing the sample at the stage. The side of sample which was symmetrical was faced towards stage while other face of sample was cover with the powder. Polymeric powder called phenolic resin was used. A temperature of 174 °C and a force of about 250 bar was applied during the embedding of the specimen. Timer was set for 25 minutes. After 25 minutes, heater was tuned off, pressure was released, and water cooling was used to obtain the shortest possible mounting time.

b) Grinding

Grinding was performed to improve the surface finish and to remove impurities present on the surface of substrate by removing a small amount of material from surface.

Grinding machine (FORCIPOL 2V) was switched on by connecting cable to the board. Emery paper of minimum grit size (P220) was selected and fixed in grinding machine and water was allowed to fall on sandpaper. Grinding machine was turned on by pressing start button and speed was adjusted accordingly (between 100 to 200 rpm). When machine was turned on. Emery paper started to rotate. Sample were pushed (by applying force) on rotating disc horizontally for 10 minutes approximately. Direction of sample was changed by 90° after a little while to remove the lines on surface of sample facing the disc. This process was repeated for 5 to 10 minutes again and again by changing emery papers ranging from 220 to 2000 grid size. After that polishing was performed.

c) Polishing

Polishing was performed to enhance the appearance of substrate, to prevent contamination, to remove oxidation and to create a reflective surface. Polishing machine (Nano 1000T) was switched on by pressing start button and alumina solution was put on rotating disc of polishing machine. We turned the machine on after polyester cloth was adjusted on the rotating disc by pressing start button. Sample surface was pushed on rotating polyester cloth horizontally until mirror like surface appeared (20 minutes approximately). After that washed the sample with DI water and dried with the help of blower. After that sample was ready for other processes.

d) Demounting

Mounting of sample was break by using hammer. Force was applied in the vertical direction and sample sheet was took out again.

e) Washing

Required equipment for all processes (beaker, stirrer, pipette, tweezers, spatula, counter electrode) and samples were washed separately with equal ratio of DI-water and cleaning ethanol and dried before use.

3.3. Synthesis of TNTs

TNTs were synthesized by means of electrochemical anodization process which consists of an electrolyte and two electrodes as show in fig.3.2. Solution of electrolyte was prepared from Ammonium fluoride, ethylene glycol and deionized water [48][47][49]. To make an electrolyte 50 mL suspension was prepared.

1st Step: 0.15 g Ammonium fluoride was added into 1.5 mL (3 vol.%) deionized (DI) water in 50 mL beaker with continuous magnetic stirring (MS-H280-Pro) until it gets completely dissolved into DI water [47][53].

2nd Step: Then 48.5 mL (97 vol.%) ethylene glycol was added into the solution with continuous stirring for 15 minutes. The purpose of using organic solvent is to prevent hydrolysis. When we apply electric field there are chances of hydrolysis, oxygen may get evolved and moves towards anode which causes bubbling and gas entrapment [48][53][54].

3rd Step: Once electrolyte was prepared, a complete cell was made. For that purpose, at anode titania was used as a working electrode and at cathode stainless steel was used as an opposite electrode with an interspacing of 10 mm, connected with power supply at 20 V and then completely dipped the electrodes into an electrolyte for 2 hours at room temperature [53][54][55].

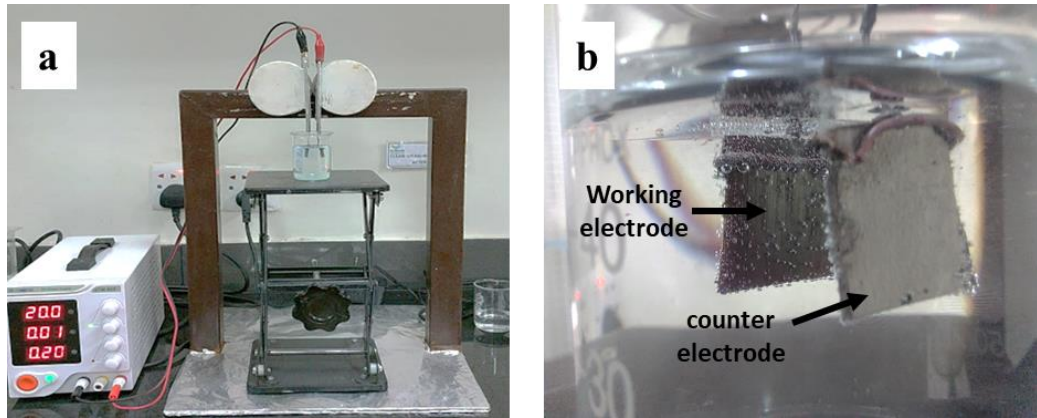


Fig 3.2. Electrochemical anodization setup for the synthesis of TNTs

When current passes ammonium and fluoride ions get separated. After that Fluoride ions will start reacting with the compact surface of titania and results in forming titanium fluoride. When titanium reacts with the fluoride ions it gets neutralized and leaves the surface and entered the solution which leaves pores in the substrate and leads to create tubes by further oxidation because there are more chances of growing tubes at the pore sites. These tubes are then further loaded by nanoparticles by means of electrophoretic deposition process as shown in fig 3.3 [56][57].

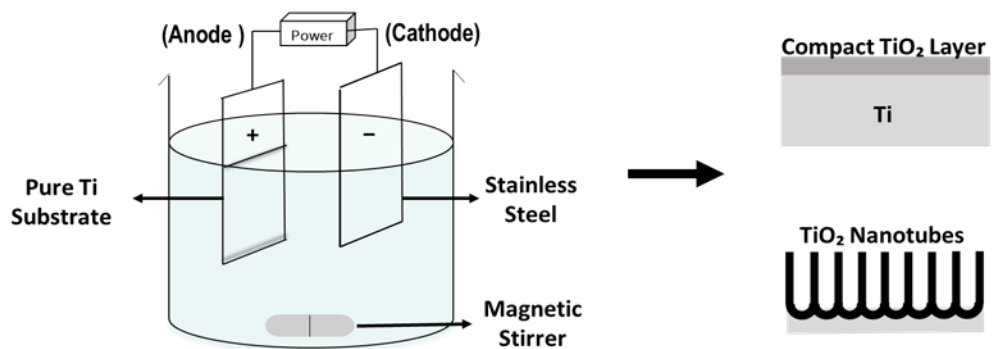


Fig 3.3. Process for the synthesis of TNTs

3.4. Annealing of TNTs substrate

After the synthesis of TNTs, substrate was annealed at 500 °C (5 °C per minute) for 4 hours in tube furnace (KJ-1600VF) in the presence of Argon gas environment to remove stresses generated due to the formation of TiO₂ layer etcetera [58].

3.5. Synthesizes of mesoporous bioactive glass Nanoparticles

1st Step: For the synthesis of mesoporous bioactive glass nanoparticles Bano et al. [52] was followed. 104 mL DI water was measured with the help of pipette in glass bottle/ flask and 2.24 g CTAB surfactant was added by measuring on weighing balance (BM-320). Place the glass bottle/ flask on Magnetic stirrer (MS-H280-Pro) at 200 rpm for 30 min at 30 °C [52].

2nd Step: After 30 minutes heat was turned off when foamy appearance occurred and 32 mL ethyl acetate with the help of pipette was added at room temperature, the solution appeared clear.

3rd Step: After 30 minutes 22 mL (28%) NH₄OH (0.5 mL NH₃ + 28 mL DI water (pH 10.5)) with the help of pipette was added due to which pH of mixture was decrease to 9.2.

4th Step: After 15 minutes of stirring, 23.04 mL TEOS was added dropwise via burette. Then after 30 minutes stirring 5.21 g (30%) CaNO₃ was added with the help of spatula.

5th Step: After 4 hours stirring, the suspension was leaved overnight and then centrifuged (BKC-TH16) at 9000 rpm for 10 min and washed with DI water for three times and with washing ethanol (30 % pure ethanol-70 % DI water) for three times at 9000 rpm for 10 minutes.

6th Step: Particles were kept in incubator (WT-303-OS) for 24 hours at 60 °C for drying as described in fig 3.4.

7th Step: Then MBGNs were grinded after taking out from incubator to get powder form of nanoparticles.

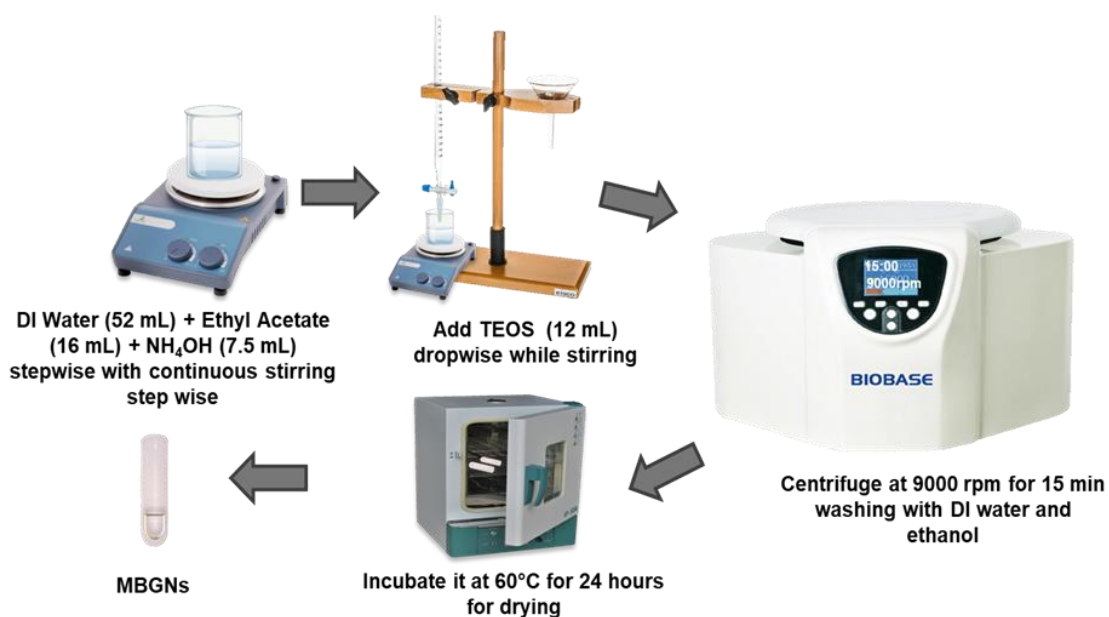


Fig 3.4. Process for the synthesis of MBGNs

3.6. Synthesizes of Zein NPs

For the synthesis of zein NPs we have prepared 50ml suspension with 4:1 ratio of ethanol and DI water, and 1 g zein powder as described in fig 3.5 [59][60][61].

1st Step: At first, 40 mL ethanol was taken in 50 mL beaker and then 1 g zein powder was weighed and added into the beaker. Place the beaker on magnetic stirrer for at least 3 hours at 500 rpm.

2nd Step: Then 10 mL DI water was added with the help of pipette and ultrasonicated (FSF-020S) for 30 minutes.

3rd Step: After 30 minutes of ultrasonication again the suspension was magnetically stirred for 3 hours to get homogeneous suspension.

4th Step: Solute precipitates present in the suspension led to the formation of nanoparticles with the help of ultracentrifugation at 3000 rpm for 15 minutes. After that

zein nanoparticles were washed with DI water and ethanol in centrifuge at 3000 rpm for 15 minutes.

5th Step: After that, nanoparticles were collected and leaved for drying in incubator for 24 h at 60 °C [50].

6th Step: Then nanoparticles were grinded in the powder form to use for further process.

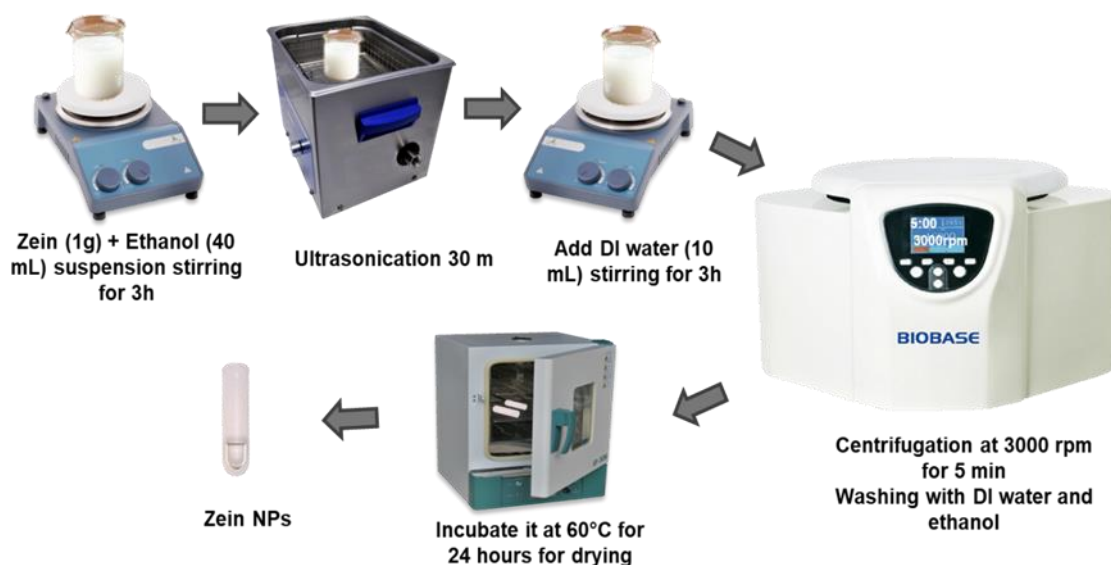


Fig 3.5. Synthesis of zein NPs

3.7. Preparation of herb

Initially, herb purchased from local market was in the form of solid accumulated grains as shown in fig 3.6 (A) because of the presence of gum resin in it which is difficult to dissolve in the suspension. Therefore, at first, we left the herb to get dried in the natural air in case of any moisture content is present. After that grinded the herb manually and used its powder form as in fig 3.6 (B).

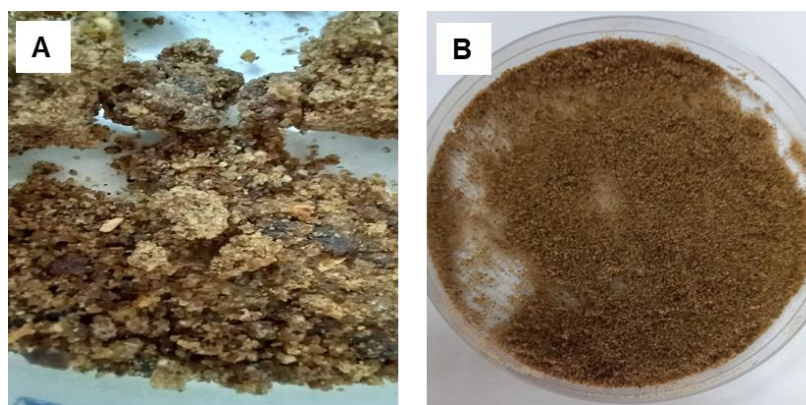


Fig 3.6. (A) Gum resin (B) Powder of *Commiphora Wightii*

3.8. Suspension preparation

For electrophoretic deposition first we had prepared suspension with pH 2.8 including mesoporous bioactive glass nanoparticles, zein nanoparticles and *Commiphora Wightii* which needs to be deposited on the substrate with the composition obtained by Batool et al. [50] using Taguchi DoE.

1st Step: For the preparation of 50 mL suspension, 2 g Zein NPs were mixed with 10 ml acetic acid with continuous magnetic stirring at 300 rpm. After 30 minutes the suspension was ultrasonicated for 10 minutes. pH and temperature of the suspension was checked after each step using pH meter (HI 2211 Ph/ORP Meter) [59].

2nd Step: Again, the suspension was put back on to the magnetic stirrer and 0.2 g MBGNs were added to the suspension. Again after 30 minutes suspension was ultrasonicated for 10 minutes [62].

3rd Step: After that 0.1 g of *C. wightii* was added into suspension again with continuous stirring.

4th Step: After 1 hour of stirring 3 mL Deionized water was added again with continuous stirring.

5th Step: And finally, 37 mL of ethanol was added after 1 hour of stirring again. After adding ethanol suspension was left to stir for 3 to 4 hours to get a stable suspension. After that suspension was sonicate for about 20 – 30 minutes. Again, stir the suspension for 15-20 minutes before setting up the EPD process if possible as described in fig 3.7 [62].

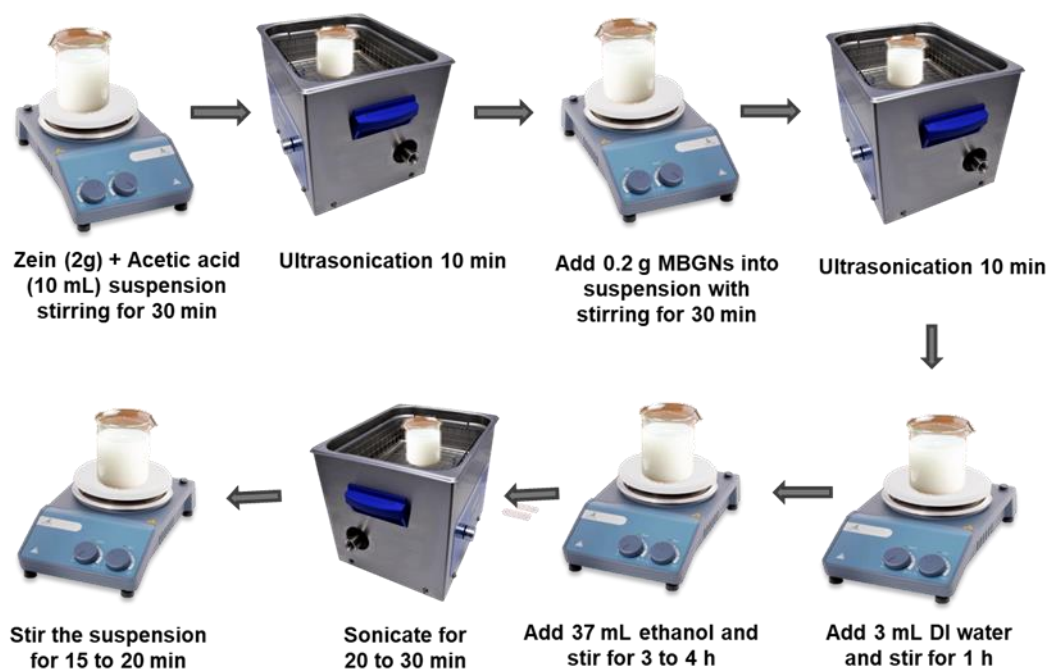


Fig 3.7. Process for suspension preparation

3.9. Electrophoretic deposition of Zein NPs/MBGNs/ *C. wightii* on TNTs

After the synthesis of nanoparticles, we will do coatings by means of cathodic EPD process due to its cost effectiveness, versatility since it can be modified easily for any specific application and relatively simple apparatus operative at room temperature. Basically, in EPD process pure titanium is used as a working electrode and SS as an anode so when electric field is applied then powder particles dispersed in the liquid medium get positively charged and attract towards cathode and get deposited on the Ti substrate as described in fig 3.8 [32].

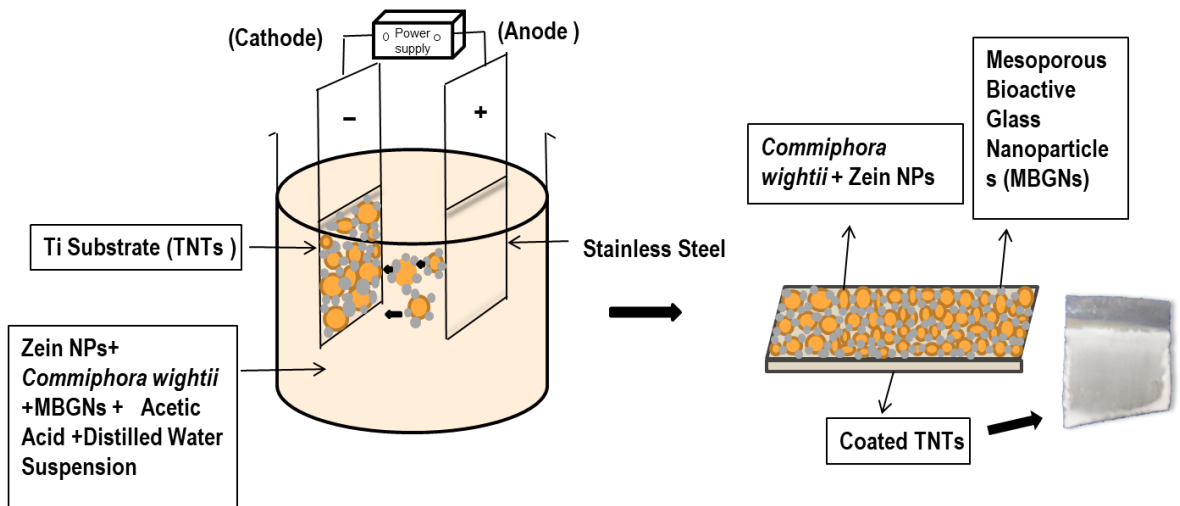


Fig 3.8. EPD process

Once the suspension was prepared with pH 2.8, its stability was checked by depositing it by means of electrophoretic deposition due to its cost effectiveness, versatility since it can be modified easily for any specific application and relatively simple apparatus operative at room temperature. Stainless Steel substrate was set as both working electrode and anode with an interspacing of 10 mm and voltage supply of 20 V for 5 minutes. There are the parameters already obtained for Stainless Steel by using Taguchi design of experiment approach [63]. But these parameters are for Stainless Steel which has different conductivity as compared to the Titanium and for annealed titanium, due to the presence of nanotubes, more coating time and voltage was required because the suspension will fill the nanotubes first and then adhere as coating on the surface of the substrate. Therefore, main problem occurred here that how many volts will be applied and for how much time to get uniform deposition.

By taking an idea from Taguchi DoE it was obtained that applied voltage, and time are the main parameters that effect the deposition rate on a large scale. We can easily control thickness and morphology of our deposited film by simply adjusting the parameters. To make a complete cell titania nanotubes substrate was tied with stainless

steel sheet by means of copper wire to enhance its conductivity at cathode and Stainless Steel was used as an anode as well. Both electrodes connected with power supply and then dipped into the suspension.

After that trial error approach was used to carry further experimentation. Number of experiments were carried out at different voltages and times.

Table 3.1. Trial-Error Approach Parameters

Run	Voltage (V)	Time (min)	Run	Voltage (V)	Time (min)
1	15	5	13	35	5
2	15	7	14	35	7
3	15	10	15	35	10
4	20	5	16	40	5
5	20	7	17	40	7
6	20	10	18	40	10
7	25	5	19	45	5
8	25	7	20	45	7
9	25	10	21	45	10
10	30	5	22	50	5
11	30	7	23	50	7
12	30	10	24	50	10

When electric field was applied, and powder particles dispersed in the suspension get deposited on the titania nanotubes substrate. It was observed that no uniform coatings were obtained on all these parameters except 45 Volts for 7 minutes which was selected to carry out further processes as shown in fig 3.9.

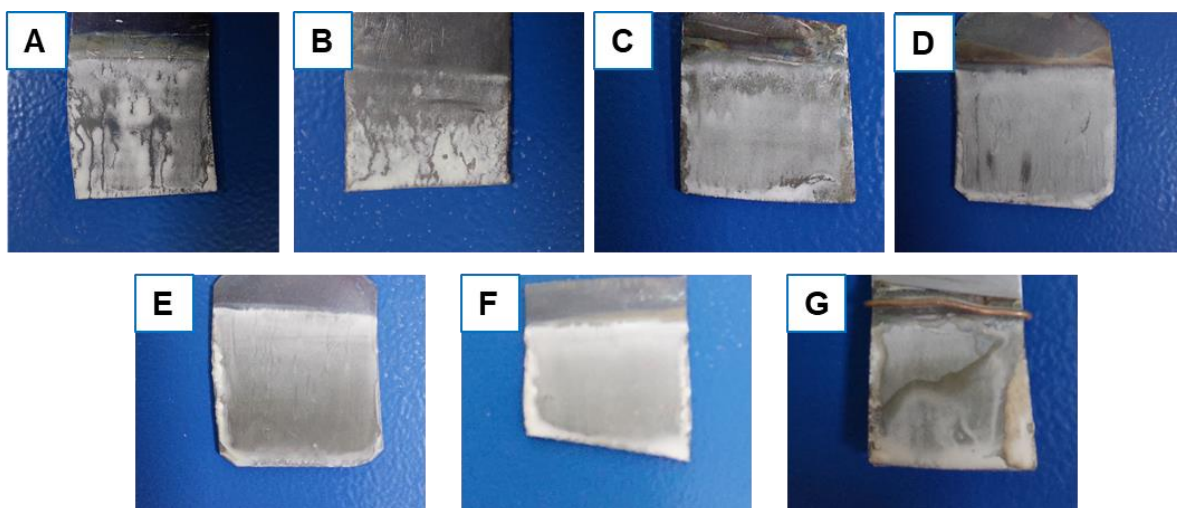


Fig 3.9. Coatings deposited at (A) At 25 V for 7 min (B) At 30 V for 7 min (C) At 35 V for 7 min (D) At 40 V for 7min (E) & (F) At 45 V for 7 min (G) At 50 V for 5 min

a) Morphological Analysis

To observe the morphology of samples field emission scanning electron microscopy (FE-SEM, MIRA 3, TESCAN) along with energy dispersive x-ray spectroscopy (EDS) was performed. For the observations of samples under SEM or to perform EDS, sample preparation is very necessary. Two different methods were used in this research work for the preparation of samples. One for the metallic sheet samples with or without coatings and other for the particles.

Sample preparation: Metallic sheet samples were prepared by simply attaching carbon tape on the studs and then sample was placed on the carbon tape and further secured with the copper tape. For the preparation of nanoparticles, we took nearly an amount of 1 mg of powder and dissolve it in 2 mL ethanol in glass tube. After that prob sonication was performed for 20 minutes and took minimal amount of liquid with spatula and spread it on the sterilized 1 cm × 1 cm glass slides gently. After that glass slide was place onto the carbon tape attached with the stud and secured with copper tape. Plasma

sputtering was done of non-conductive samples like nanoparticles and coated samples for making their surface conductive to produce high-resolution images.

Studs were placed in the scanning electron microscope with the help of tweezer and the door was closed. After that high vacuum was created into the microscope and an electron beam produced from an electron source because of thermal energy which interacts with the surface of substrate that gives topographical information of surface and the elemental composition of substrate by means of energy dispersive x-rays paired with scanning electron microscopy.

Structural analysis: To check the further chemical composition of nanoparticles, herb, bare Ti substrate, anodized (TNTs) substrate, annealed substrate, and Zein NPs+ MBGNs+ *Commiphora Wightii* coated substrate Fourier transformation infrared (ATR-FTIR, Thermofisher Nicolet Summit Pro) spectroscopy was performed. At first, sample platform and knob were cleaned with 99 %- ethanol properly and OMNIC paradigm software which is connected to FTIR was run and background noise was remove. After that, sample was placed gently with the help of spatula on the crystal of platform and screw down the knob right above to the sample. Sample scanning was started in the absorbance mode. After measurements, screw was loosed, and knob was unwound. Sample was collected and platform/knob was cleaned again with ethanol with the help of tissues.

c) Brunauer-Emmette-Teller (BET) Analysis

Brunauer-Emmette-Teller (BET) Analysis (GOLD APP, V-Sorb 2800, China) was performed to check the surface area of nanoparticles. At first, it was necessary to make nanoparticles impurities and free if any present. For which degassing was done at high temperatures in vacuum that could not affect the structure of nanoparticles. There are two chambers in BET, one is for degassing and the other is for analysis in which we

performed other processes to get the surface area. In a glass rod 0.5 g powder was kept into the chamber which has two gas inlets one is of nitrogen and other for helium. Nitrogen gas get adsorbed into the porous nanoparticles when liquid nitrogen was introduced which lowers the temperature and helps nitrogen gas to settle down. When liquid nitrogen was removed, temperature goes up and nitrogen gas was desorbed. After that desorbed gas was measured by its software further which calculates surface area and gave us different type of isotherms depend on the pore size of particles [64].

d) Surface chemistry

To determine the surface properties of composite coated samples some tests were performed.

Wettability testing: Wettability test was performed to check the nature of coatings by simply pouring 5 μ L drop of Distilled water with the help of microliter pipette on both bare Titanium substrate and Zein NPs+ MBGNs+ *Commiphora Wightii* coated substrate at different sites. After 5 seconds we took pictures of drops vertically one by one by adjusting camera at the same level of drop and measured the contact angle of that drop with both bare and coated surface using ImageJ™ software.



Fig 3.10. Contact angle measurement (wettability testing)

Surface roughness: Surface roughness of coated sample was checked via profilometer. Coated sample was put on the glass slab and a line of almost 1 cm was drawn by moving

the tip of profilometer over the coated surface which gave us an average roughness value. This test was performed three time. After that an average value of average roughness was calculated.

e) Adhesion testing

Pencil Testing: Adhesion test was performed on Zein NPs+ MBGNs+ *Commiphora Wightii* coated by standardized pencil test according to the ASTM (D3363-20) [65] to check adhesive strength of composite coatings by using different grades of pencils from hardest (2H) to softest (8B) for marking lines on the coated titania nanotube substrate.

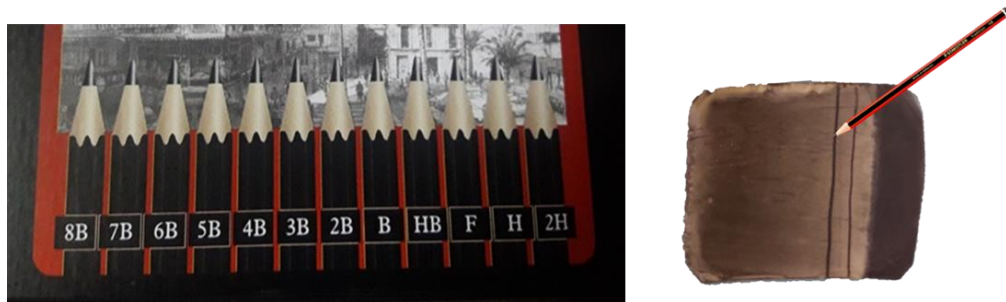


Fig 3.11. Pencils according to ASTM standards

Sample was putted over some horizontal slab and a line was marked with the sharp tip hardest grade 2H pencil lead from start to the end on the coated sample. This procedure was continued with other pencils until the coatings got scratched or removed for which sample was examined under optical microscope.

Cross-cut Tape Testing: To check further adhesion of coatings Cross-cut tape test was done according to the ASTM (D3359) [66] was performed by putting sample on some horizontal slab and then drawing cross hatch with the cutter on the coated substrate and the sample was examined under optical microscope to check whether any particles of coatings got scratched or removed. After that adhesive tape was applied on the coated surface where cross hatch was drawn and pulled with the force. After that again the

sample was examined under optical microscope to check the condition of coating. Figure 3.12 depicts the ASTM standard for comparing the adhesion strength of coating.

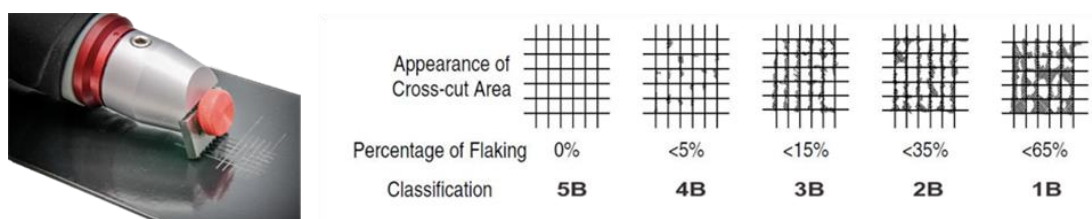


Fig 3.12. Process for cross-cut tape test by using a cutter

f) Nanoindentation

To check the further hardness profile of Zein NPs+ MBGNS+ *Commiphora Wightii* coatings on annealed substrate nanoindentation test was performed by using diamond like tip (Berkovich) indenter. Sample was placed over the stage and 3.2 mN load was applied and hold until the tip penetrates deep into the coatings and touches the substrate. After that unload and remove the sample.

g) Wear testing

Wear testing was performed on Zein NPs+ MBGNS+ *Commiphora Wightii* coated surface under moisture free conditions at room temperature by using Tribometer (MT/60/NI, Spain) to check the wear rate of coatings. A Stainless-Steel ball indenter with diameter of 6 mm was used to apply load of 1N with sliding distance of 50 m at 30 rpm.

h) Corrosion Testing

Corrosion test was performed to check whether coated layer of Zein NPs+ MBGNS+ *Commiphora Wightii* will provide corrosion resistance to the substrate or not. Potentiodynamic polarization scanning system was used to study the corrosive behavior of samples on scanning rate of 25 mVs^{-1} within $\pm 500 \text{ mV}$ potential range. This test was

performed in an electrolyte of simulated body fluid (SBF) at human body temperature 37 °C in Gamry apparatus (reference 600) which consists of three electrodes. AgCl/Ag was used as reference electrode along with graphite as counter electrode while annealed and coated samples were used as working electrodes between reference and counter electrode. At first, for 30 minutes an open circuit potential (OCP) was run. After that, values of corrosion current density (I_{corr}) and corrosion potential (E_{corr}) was determined by plotting Tafel region. Cross sectional point of both tangents of anodic and cathodic curves gave us I_{corr} value at x-axis and E_{corr} at y-axis.

i) Antibacterial testing

To check the antibacterial activity of samples disk diffusion tests were performed. Nutrient agar (Acumedia, UK) was prepared by dissolving 7 g of Nutrient agar in 250 mL Distilled water. Prepared media was then autoclaved at 121 °C for 15 minutes for the purpose of sterilization. 15 mL of agar was poured in each petri dish and was allowed to solidify at room temperature. After that drop of 20 μL of bacterial culture of both Pathogenic bacterial strains (IDC, Islamabad) with OD 0.015 was poured on two different agar plates with microliter pipette and then spread with glass spreader to make a uniform bacterial lawn and samples disc were placed. Then disks were sealed with plastic wrap and placed in the incubator (WT-303-0S) at 37 °C for 24 hours. After 24 hours disks were taken out of the incubator and results were observed.

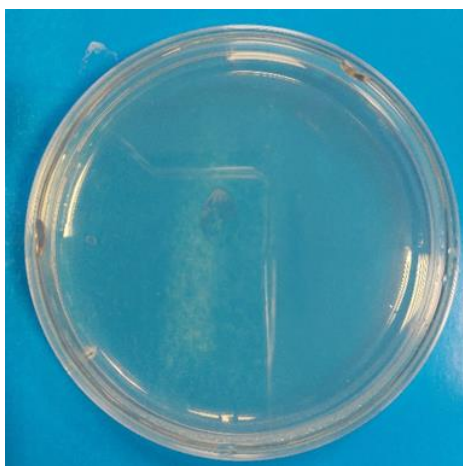


Fig 3.13. Disks prepared for disk diffusion test

j) Bioactivity testing

For testing the bioactive nature of our coated titania nanotube substrate, bioactivity testing was performed by immersing our coated samples in the simulated body fluid made in the lab by following kokobu's recipe [67] consists of the composition of salts present in the human body fluid plasma pH 7.4 at 37 °C (checked by using pH meter) in the 20ml falcon tubes for different days (1,3,5,7,14). Falcon tubes were placed in the shaking incubator (BJPX 0 B) at 37 °C on 80 rpm after immersing the samples in it. After the completion of these days, we took our samples were took out and washed with deionized water, dried with drying machine, and SEM was performed.

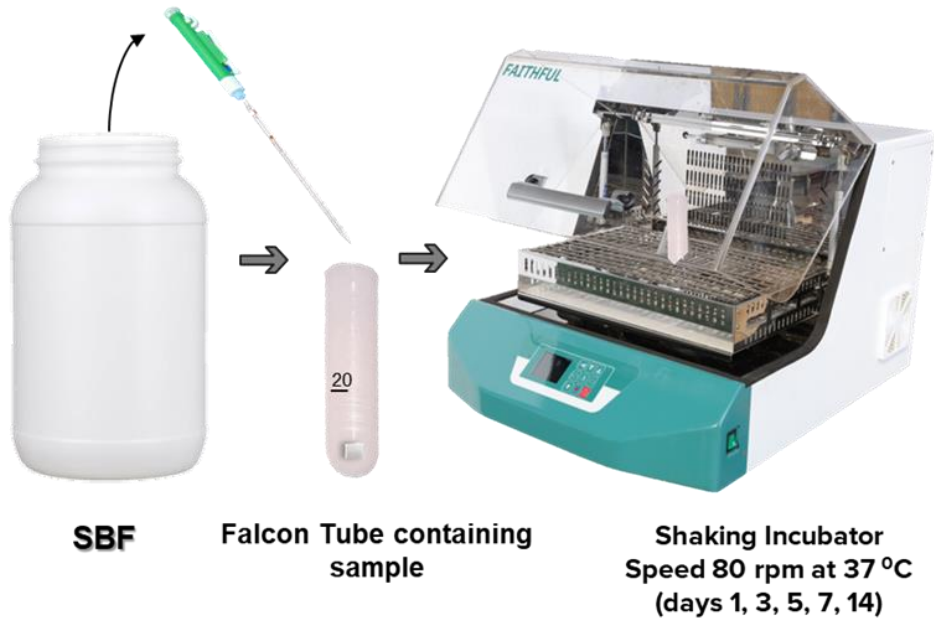


Fig 3.14. Bioactivity testing of synthesized coating in SBF

4. RESULTS & DISCUSSIONS

4.1. Materials Characterization

a) SEM/EDX of materials

i. TNTs

TNTs were synthesized over the titanium substrate by electrochemical anodization process with optimized parameters explained in chapter 3. Figure 4.1 A shows the SEM image of TNTs at the surface. It can be clearly seen that the nanotubes are uniformly distributed over the titanium substrate. The diameter across all nanotubes also looks very uniform. The average diameter calculated from the SEM software was 40 ± 3 nm. Figure 4.1 B shows the SEM image of cross section of TNTs sample. The average depth (length) of TNTs was $308.17 \mu\text{m}$. EDX of TNTs sample in figure 4.1 C confirmed the presence of Ti and O, compositions are shown in table 4.1.

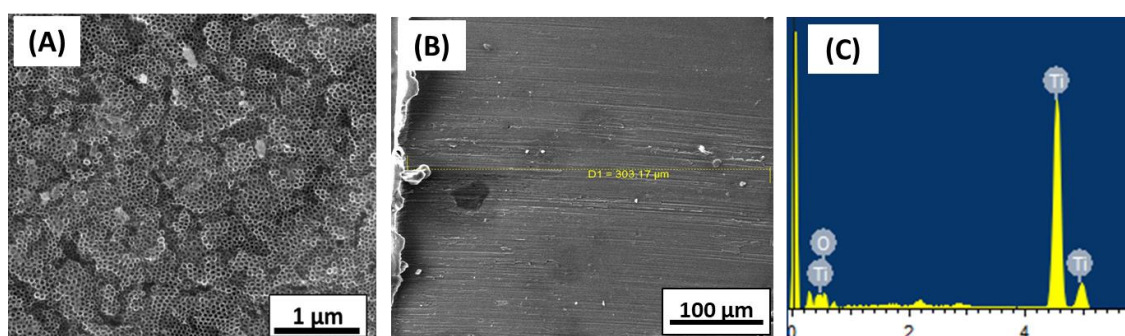


Fig 4.1. (A) SEM Image of TNTs Surface (B) Cross section of TNTs (C) EDX spectrum

Table 4.1. EDX Composition of TNTs (wt% and at%)

Element	Weight %	Atomic %
O K	28.35	54.22
Ti K	71.65	45.78

Total	100	100
--------------	-----	-----

ii.MBGNs

MBGNs were synthesized by modified Stober process as explained in Chapter 3. Figure 4.2 (A) shows the SEM image of MBGNs. The average particle size was 140 ± 18 nm. Particles had a rough / porous surface, which corresponds to mesoporosity. Mesoporosity is in the range of 2 – 50 nm. Figure 4.2 (B) shows the EDX spectrum showing elements present in MBGNs i.e., Si, O and Ca. Their elemental composition is given in table 4-2.

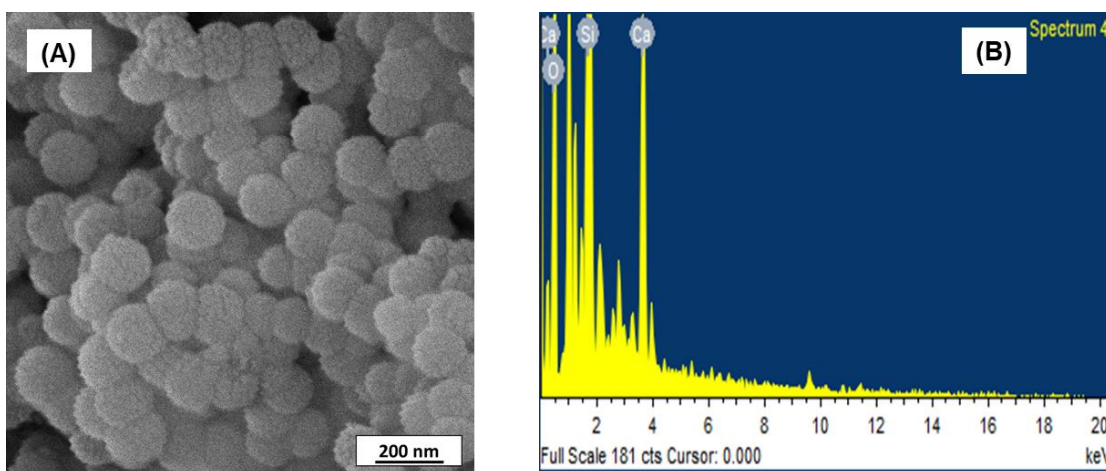


Fig 4.2. (A) SEM Image of MBGNs (B) EDS spectrum

Table 4.2. EDX Composition of MBGNs (wt% and at%)

Element	Weight %	Atomic %
Si K	50.42	65.14
O K	42.18	31.04
Ca K	7.40	3.82
Total	100	100

b) BET of MBGNs

Figure 4.3 shows BET graph of MBGNs showing Type IV isotherm, which represents mesoporosity (2 – 50 nm range). Surface area was 196.7 m²/g.

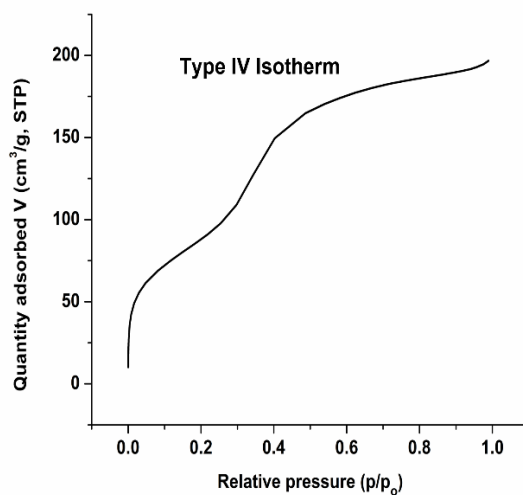


Fig 4.3. BET Graph of MBGNs

Zein nanoparticles were synthesized via solvent evaporation method, explained in detail in chapter 3.

Figure 4.4 shows SEM image of zein NPs. Average particle diameter was 157 ± 25 nm. Composition was confirmed in figure 4.4 and table 4-3, showing presence of O and C, major constituents of Zein.

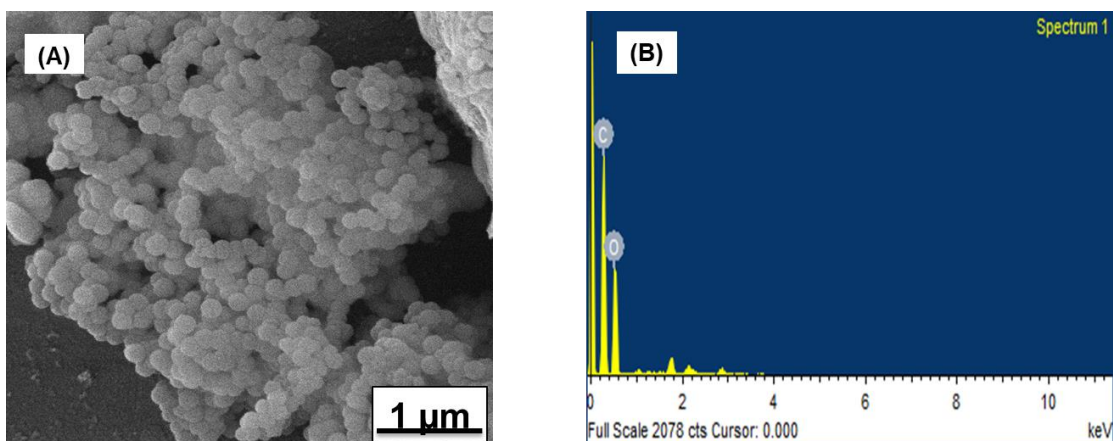


Fig 4.4. (A) SEM of Zein NPs (B) EDX spectrum

c) BET of Zein NPs

Figure 4.5 shows BET graph of Zein NPs showing Type II isotherm, which indicated that there is no porosity in the Zein particles. Surface area was 35.2 m²/g.

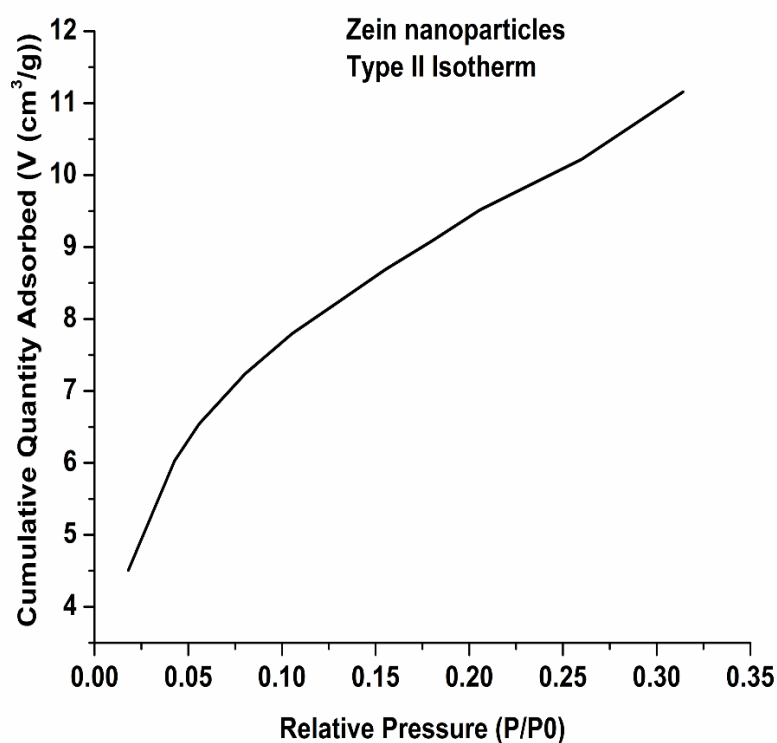


Fig 4.5. BET Graph of Zein NPs

Our herb, *C. wightii*, was bought in Gum resin form from local pansari shop. It was later crushed and dried to get powder form. Antibacterial effect of our herb *C. wightii*

was confirmed via disk diffusion test. Three different concentrations of herb were prepared in ethanol to check the MIC. These concentrations were 0.1 g herb in 10 mL ethanol, 0.01 g herb in 10 mL ethanol, and 0.001 g herb in 10 mL ethanol.

In *S. aureus* medium, the inhibition zones obtained for 0.1 g, 0.01 g, and 0.001 g herb were 14 mm, 4 mm, and 3 mm respectively. In *E. coli* medium, the inhibition zones obtained for 0.1 g, 0.01 g, and 0.001 g herb were 10 mm, 6 mm, and 3 mm respectively.

Results are shown against control sample (0 g herb) in figure 4.6.

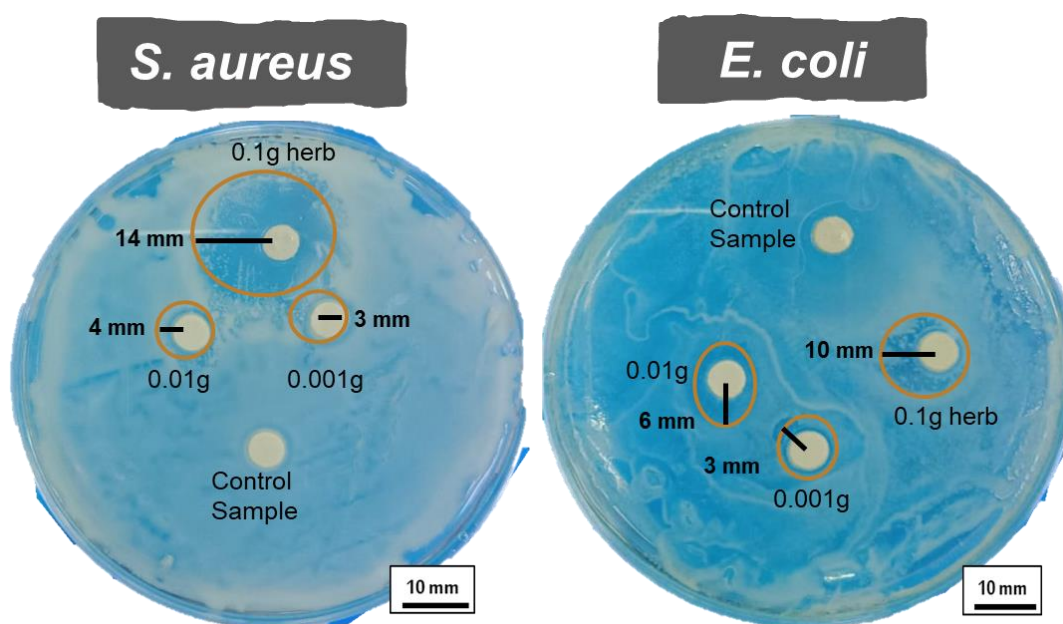


Fig 4.6. Antibacterial Test (Disk Diffusion) for *C.wightii* in different concentrations against *S.aureus* & *E.coli*

d) FTIR of Materials

Figure 4.7 shows FTIR of Zein NPs, MBGNs and our Herb. Peak at 3300 cm^{-1} shows presence of OH group due to moisture content. Peak at 2800 cm^{-1} shows presence of Alkane groups. Peak at 1600 cm^{-1} shows the presence of carbonyl group. Peak at 1200 cm^{-1} shows the presence of amide groups. And peak at 1000 cm^{-1} shows the presence of cyanide group. All these groups are constituents of zein. Peaks at 600 cm^{-1} and 1000 cm^{-1} show the presence of Si-O (silica) bonds. These types of bonds constitute MBGNs.

Peak at 2300 cm^{-1} shows the presence of phosphine group. Peak at 1000 cm^{-1} shows the presence of esters. Along with peaks of hydroxyl, alkanes and amides, these groups are constituents of the herb *C. wightii*.

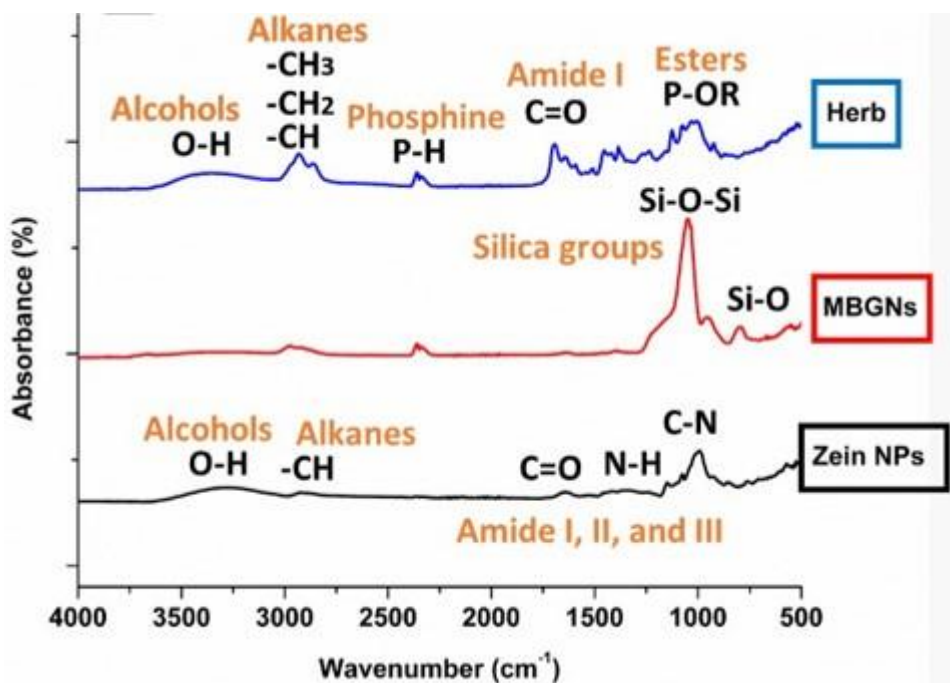


Fig 4.7. FTIR of Zein NPs, MBGNs, and Herb

We obtained our composite coating on TNTs sample via EPD process at optimized parameters explained in chapter 3.

a) SEM/EDX

Figure 4.13 shows the SEM image of surface of the coating. Figure 4.14 shows the SEM image of cross section of coating. The average thickness was $22\ \mu\text{m}$. Figure 4.15 gives the elemental mapping of the coating which shows different elements present in the coating represented by different colors. Table 4-3 shows compositions of these elements.

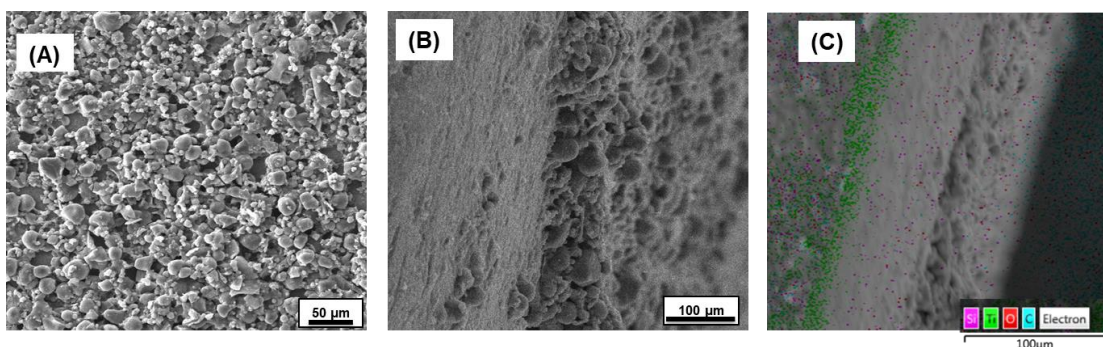


Fig 4.8. (A) SEM Image of coating surface (B) SEM of coating thickness (C)

Elemental mapping of coating

Table 4.3. EDX Composition of Composite Coating

Element	Weight %	Atomic %
O K	65.14	83.11
Ti K	28.10	11.97
Si K	6.76	4.92
Total	100	100

b) FTIR

Figure 4.9 shows the FTIR of coating containing zein nanoparticles, MBGNs and herb. Different peaks were observed in the plot. Peaks around 3300 , 2800 , and 1600 cm^{-1} indicated presence of alcohol, alkane, and amide groups respectively which represent zein and herb. Peaks observed around 1000 cm^{-1} indicated presence of cyanide group of zein and ester group present in herb and silica group present in MBGNs. Peak at 2200 cm^{-1} indicated presence of phosphine group present in herb.

Table 4.4. Wave Number and related Bonds, Materials

Wave Number (cm^{-1})	Associated Bonds	Material
800	Si-O	MBGNs
1000	C-N, Si-O-Si, P- OR	Zein, MBGNs, <i>C. wightii</i>
1500	N-H	Zein
1600	C=O	Zein, <i>C. wightii</i>
2300	P-H	<i>C. wightii</i>
2800	-CH ₃ , -CH ₂ , -CH	Zein, <i>C. wightii</i>
3300	-OH	Zein, <i>C. wightii</i>

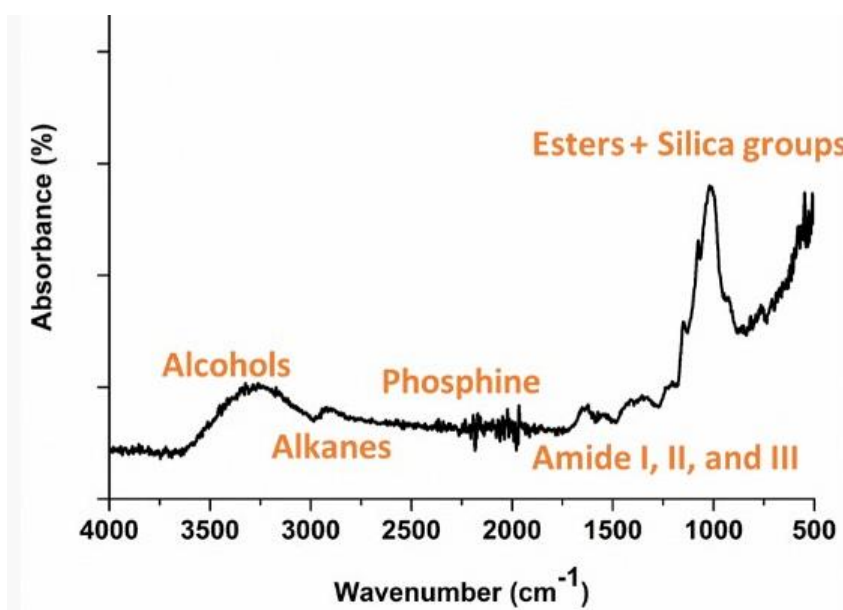


Fig 4.9. FTIR of Composite Coating

Pencil Test: Standardized pencil test according to ASTM D3363-20 was performed on the coated TNTs sample. Pencils of different grades ranging from hardness level 8B to

2H were used to mark lines over the coating. It was to see if coating wears off. The marked sample was then examined under the optical microscope. No coating was removed as shown in figure 4.10. Thus, the coated sample was labelled 2H, the hardest grade of pencil that did not scratch the coating.

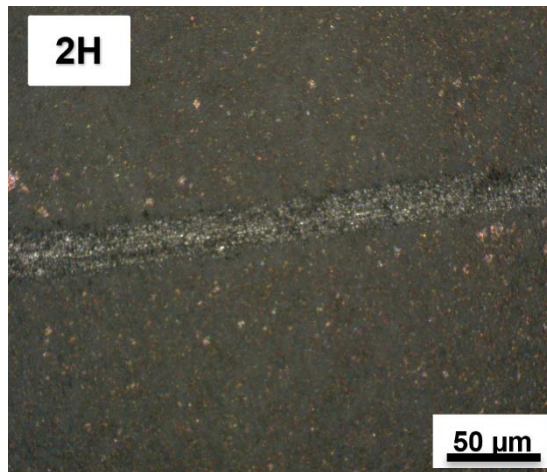


Fig 4.10. Pencil Test Result under Optical Microscope

Cross Hatch Test: To further test coating, cross hatch cutter / tape test was performed according to ASTM D335997. Cross hatch cutter was used to draw a cross hatch over the coating and examined under optical microscope. No coating got removed (Figure 4.11 (A)). Then, adhesive tape was applied over the cross hatch and removed to see if any coating removes. Sample was again observed under the optical microscope (Figure 4.11 (B)). Again, no coating was removed. Thus, 5B was labelled at the coating (0% damage).

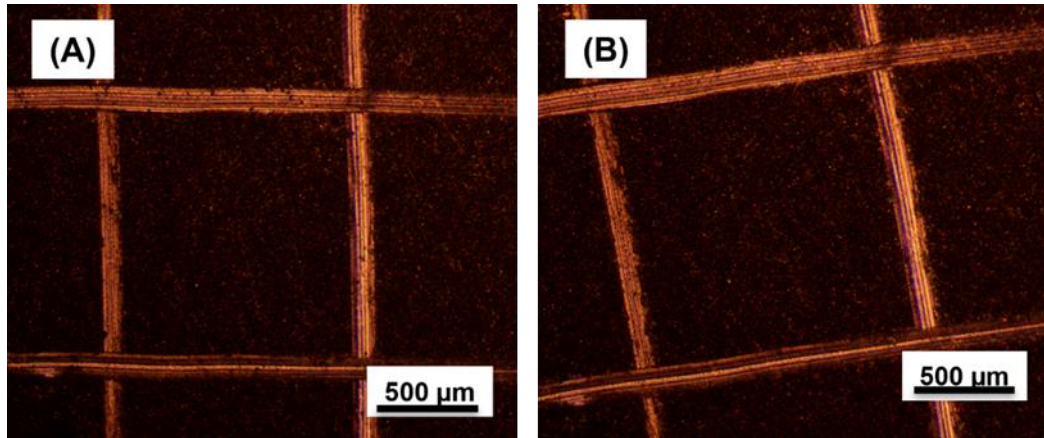


Fig 4.11. Cross hatch test (A) before adhesive tape was applied (B) after tape was applied

c) Nano Indentation

In nanoindentation graph shown in figure, mechanical properties of coating are favorable in both elastic and plastic regions.

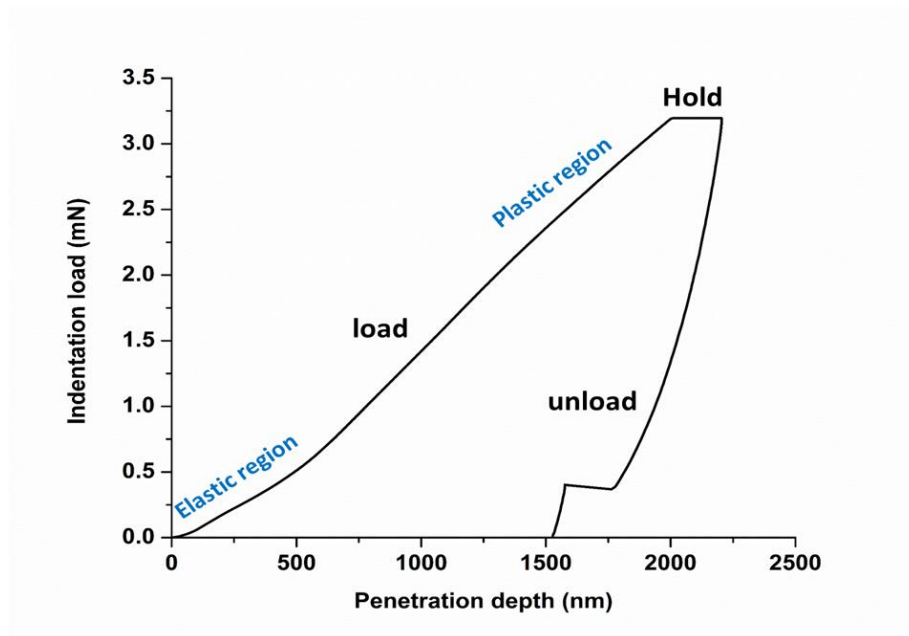


Fig 4.12. Nano Indentation graph of coating

Corrosion test was performed on the coated sample in SBF via Gamry apparatus. The graph obtained at a result (shown in figure) showed a comparison between coated sample and simple annealed TNT sample. From the graph, it was clear that corrosion density of the coated sample was less as compared to uncoated sample. Thus, the corrosion resistance of coated sample was more than that of simple uncoated sample.

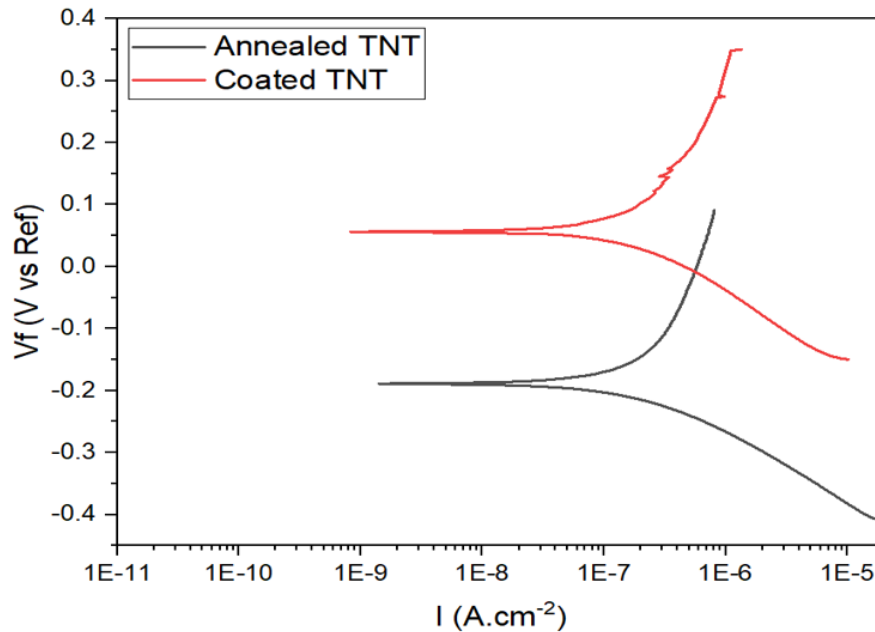


Fig 4.13. Corrosion behavior of Coated and Uncoated TNTs

Wettability: Wettability test was performed on coating to measure contact angle to determine hydrophilicity / hydrophobicity of coating. ImageJ software was used to determine the contact angle. Contact angle measured was $53 \pm 5^\circ$ for bare TNTs and $79 \pm 4^\circ$. Shown in Figure 4.14. This shows hydrophilic properties, which are suitable for protein attachment.

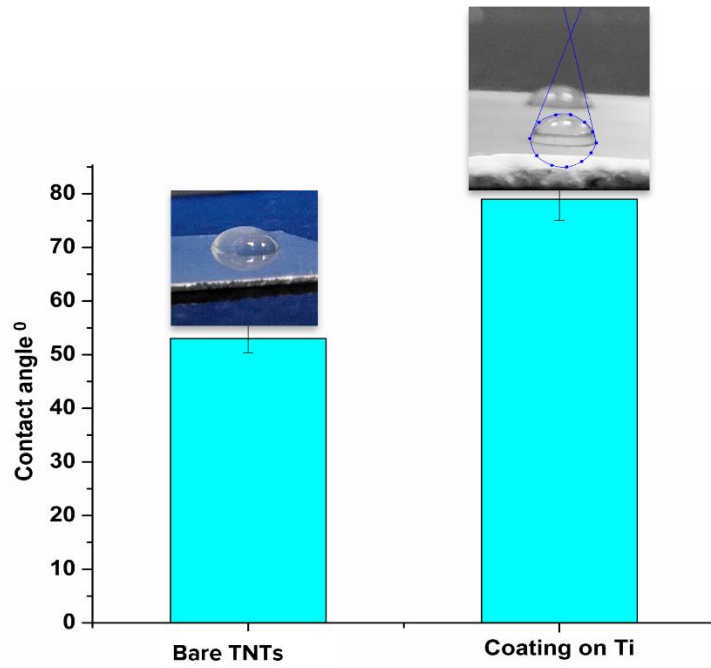


Fig 4.14. Contact Angle (Bare and Coated TNTs)

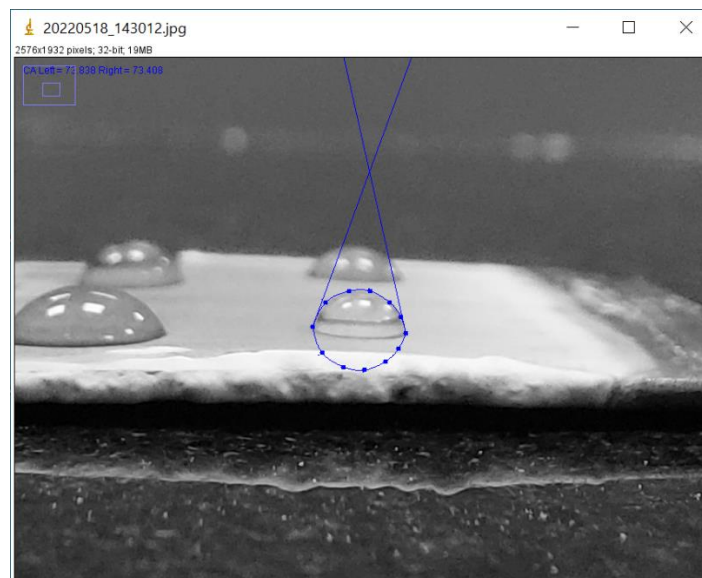


Fig 4.15. Contact Angle Measurement via ImageJ software

d) Surface Roughness

Average surface roughness was obtained at $1.2 \pm 0.03 \mu\text{m}$. Optimum value of surface roughness for protein attachment ranges from $1.2 - 2.0 \mu\text{m}$.

e) Bioactivity Test

Bioactivity / SBF test was performed on coated TNTs samples. Samples were put in SBF for 5, 7, and 14 days respectively.

When day 5 sample was analyzed under SEM, it was observed that no Phosphorus or Calcium was formed, elements that indicate presence of HA layer (formation of HA indicates bioactivity).

When day 7 sample was analyzed under SEM, it was observed that Phosphorus and calcium have formed in some quantity, indicating the formation of HA layer.

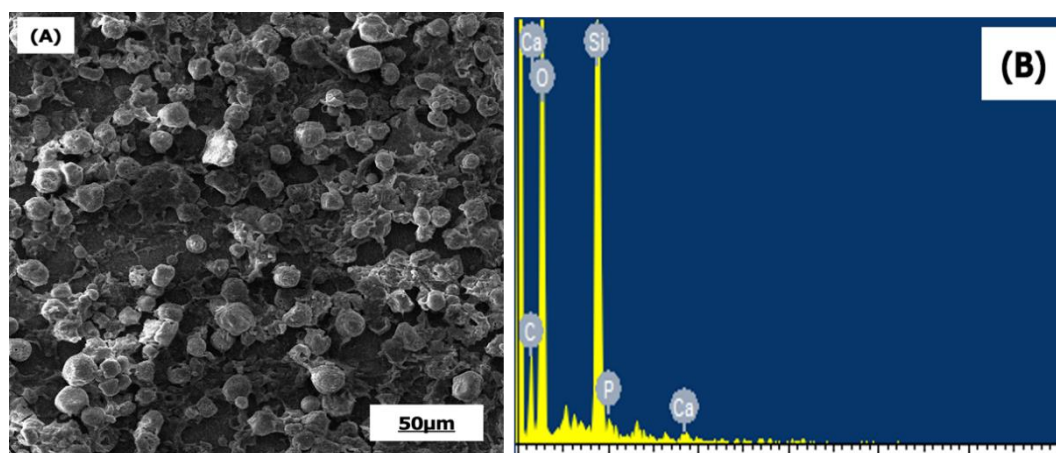


Fig 4.16. (A) SEM image of Surface (7 days) (B) EDX Spectrum of Bioactivity sample (7 days)

Table 4.5. EDX composition of 7 days sample

Element	Weight %	Atomic %
C K	14.04	20.74
O K	52.99	58.78
Si K	30.05	18.99
P K	1.53	0.88
Ca K	1.39	0.62
Total	100	100

When day 14 sample was analyzed, fully grown needles of calcium phosphate (HA layer) were observed in SEM images.

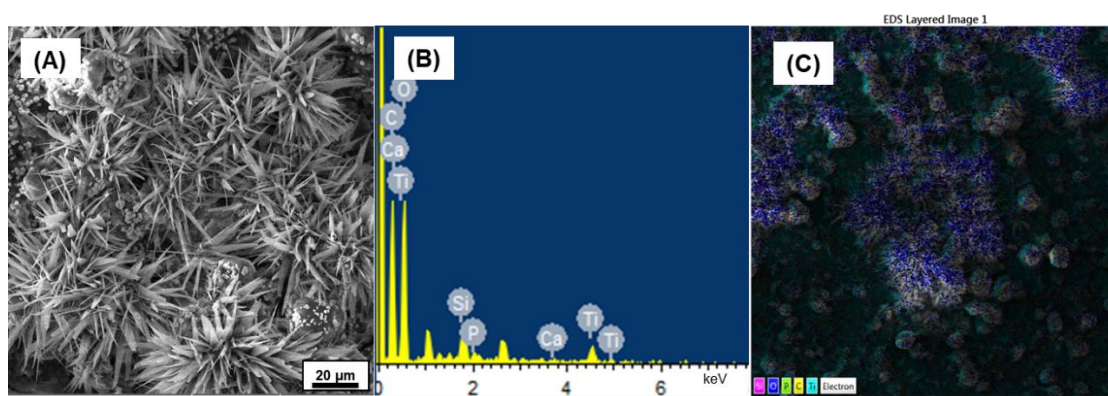


Fig 4.17. (A) Bioactivity Test, (B) EDX Spectrum & (C) Elemental Mapping of 14 Days sample

Table 4.6. EDX composition of 14 days sample

Element	Weight %	Atomic %
C	24.35	32.51
O	62.08	62.22
Si	0.34	0.20
P	2.77	1.43
Ca	2.15	0.86
Ti	8.31	2.78
Total	100	100

Antibacterial Test: Disk diffusion test was performed on our coated TNTs sample against gram-positive and gram-negative bacteria. Zone of inhibition was formed around the samples as shown in figure 4.18, confirming the antibacterial effect of coating.

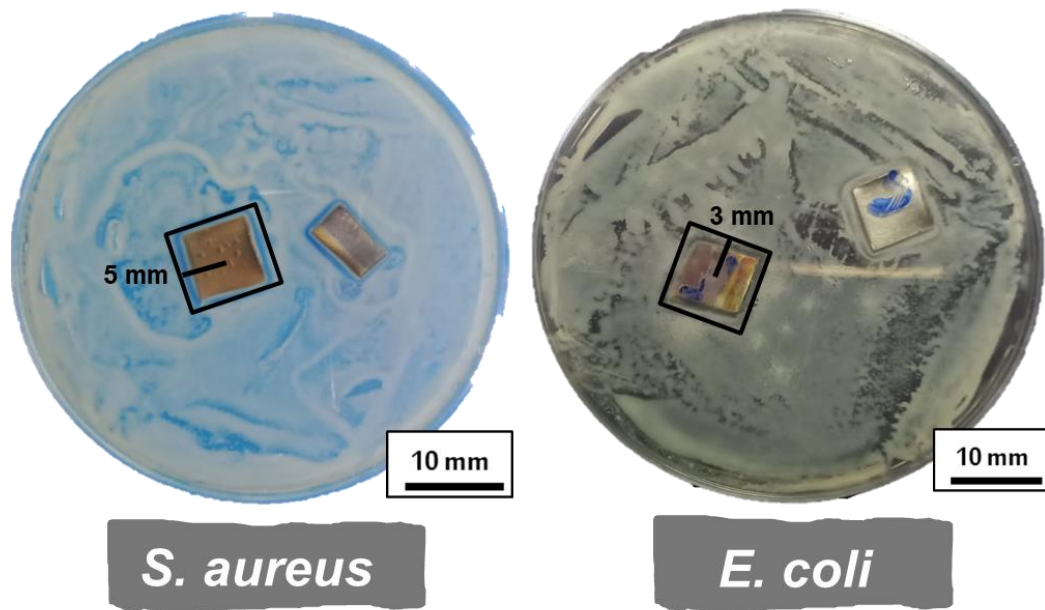


Fig 4.18. Antibacterial Test results against *S. aureus* & *E. coli*

5. CONCLUSIONS

TNTs have synthesized successfully on the titanium substrate and then nanoparticles for the composite coating also have been successfully. After that homogenous and uniform distribution of Zein NPs / MBGNs was also achieved over the substrate surface which was confirmed by SEM and FTIR results. Further adhesion strength of coated layer was also good as no particles were found removed when examined under optical microscope. Wettability and surface roughness properties were also favorable for protein attachments. Inhibition of biofilm formation due to presence of *Commiphorine* was also confirmed by antibacterial test on the coated surface. Bioactivity was also confirmed via HA layer formation in SBF at day 14.

6. FUTURE PROSPECTS

- Coatings can be examined for protein adsorption to study cell attachment process
- Zeta potential could be done which is important for charge measurement to get stable suspension
- Drug release studies could be carried out to control the release of drugs because at first burst release is required to avoid any contamination and bacterial film formation and after that sustained release of drug is required,
- Cytocompatibility of coated implant with bone cells
- If all the in vitro studies are effective in-vivo trials will also be proceeded.

REFERENCES

- [1] K. Suzuki, K. Aoki, and K. Ohya, “Effects of surface roughness of titanium implants on bone remodeling activity of femur in rabbits.,” *Bone*, vol. 21, no. 6, pp. 507–514, Dec. 1997, doi: 10.1016/s8756-3282(97)00204-4.
- [2] Biolin Scientific, “Effect of Wettability in Biomedical Applications”.
- [3] G. Manivasagam, D. Dhinasekaran, and A. Rajamanickam, “Biomedical Implants: Corrosion and its Prevention -A Review,” *Recent Patents Corros. Sci.*, vol. 2, pp. 40–54, Jun. 2010, doi: 10.2174/1877610801002010040.
- [4] D. C. Tapscott and C. Wottowa, “Orthopedic Implant Materials,” 2020.
- [5] B. P. Sharma, G. S. Rao, S. Gupta, P. Gupta, and A. Prasad, *Advances in Engineering Materials*. Springer, 2021.
- [6] S. Dolnicar *et al.*, “Scholar (3),” *Annals of Tourism Research*, vol. 3, no. 1. pp. 1–2, 2015. [Online]. Available: <http://www.sciencedirect.com/science/article/pii/S0160738315000444>
- [7] S. M. Rabiee, N. Nazparvar, M. Azizian, D. Vashae, and L. Tayebi, “Effect of ion substitution on properties of bioactive glasses: A review,” *Ceram. Int.*, vol. 41, no. 6, pp. 7241–7251, 2015, doi: 10.1016/j.ceramint.2015.02.140.
- [8] D. A. Florea, D. Albuleț, A. M. Grumezescu, and E. Andronescu, “Surface modification—A step forward to overcome the current challenges in orthopedic industry and to obtain an improved osseointegration and antimicrobial properties,” *Mater. Chem. Phys.*, vol. 243, p. 122579, 2020.
- [9] X. Li and Y. Hu, “The treatment of osteomyelitis with gentamicin-reconstituted bone xenograft-composite,” *J. Bone Joint Surg. Br.*, vol. 83, no. 7, pp. 1063–

1068, 2001.

- [10] L. C. Z. Khan, M. Arif, and R. Saqib, “Cost effectiveness of locally manufactured orthopedic implants,” *PAFMJ*, vol. 62, no. 4 SE-Original Articles, Dec. 2012.
- [11] N. Eliaz, “Corrosion of Metallic Biomaterials: A Review,” *Mater. (Basel, Switzerland)*, vol. 12, no. 3, p. 407, Jan. 2019, doi: 10.3390/ma12030407.
- [12] Z.-Y. Yuan and B.-L. Su, “Titanium oxide nanotubes, nanofibers and nanowires,” *Colloids Surfaces A Physicochem. Eng. Asp.*, vol. 241, no. 1, pp. 173–183, 2004, doi: <https://doi.org/10.1016/j.colsurfa.2004.04.030>.
- [13] A. Bandyopadhyay, A. Shivaram, I. Mitra, and S. Bose, “Electrically polarized TiO₂ nanotubes on Ti implants to enhance early-stage osseointegration,” *Acta Biomater.*, vol. 96, pp. 686–693, 2019, doi: 10.1016/j.actbio.2019.07.028.
- [14] H. I. Jaafar, A. M. A. Alsammerraei, and H. H. Hamdan, “STUDY OF THE EFFECT OF NH₄F CONCENTRATION ON THE STRUCTURE OF ELECTROCHEMICALLY PREPARED TiO₂ NANOTUBES ائنايميكورنكلا (رد ءسارينات زيكرت NH₄F مع بيكرت بيبانلا ءيونانلا ل) (ءرضحما) TiO₂,” vol. 53, no. 2, pp. 827–831, 2012.
- [15] Z. Zhang *et al.*, “TiO₂ nanotube arrays with a volume expansion factor greater than 2.0: Evidence against the field-assisted ejection theory,” *Electrochem. commun.*, vol. 114, p. 106717, 2020, doi: <https://doi.org/10.1016/j.elecom.2020.106717>.
- [16] S. Novak, U. Maver, Š. Peternel, P. Venturini, M. Bele, and M. Gabersček, “Electrophoretic deposition as a tool for separation of protein inclusion bodies

- from host bacteria in suspension,” *Colloids Surfaces A Physicochem. Eng. Asp.*, vol. 340, no. 1–3, pp. 155–160, 2009, doi: 10.1016/j.colsurfa.2009.03.023.
- [17] E. Avcu, Y. Yıldırım Avcu, F. E. Baştan, M. A. U. Rehman, F. Üstel, and A. R. Boccaccini, “Tailoring the surface characteristics of electrophoretically deposited chitosan-based bioactive glass composite coatings on titanium implants via grit blasting,” *Prog. Org. Coatings*, vol. 123, pp. 362–373, 2018, doi: <https://doi.org/10.1016/j.porgcoat.2018.07.021>.
- [18] M. Atiq Ur Rehman, F. E. Bastan, B. Haider, and A. R. Boccaccini, “Electrophoretic deposition of PEEK/bioactive glass composite coatings for orthopedic implants: A design of experiments (DoE) study,” *Mater. Des.*, vol. 130, pp. 223–230, 2017, doi: <https://doi.org/10.1016/j.matdes.2017.05.045>.
- [19] D. Meierfrankenfeld, A. Bury, and M. Thoennessen, “Discovery of scandium, titanium, mercury, and einsteinium isotopes,” *At. Data Nucl. Data Tables*, vol. 97, no. 2, pp. 134–151, 2011, doi: <https://doi.org/10.1016/j.adt.2010.11.001>.
- [20] M. Atiq, U. Rehman, and S. W. Husain, “Fabrication of Titania Nanotubes by Electrochemical Anodization and their Characterization,” no. October, 2015.
- [21] S. Nandi, B. Kundu, and S. Datta, “Development and Applications of Varieties of Bioactive Glass Compositions in Dental Surgery, Third Generation Tissue Engineering, Orthopaedic Surgery and as Drug Delivery System,” in *Biomater Appl Nanomed*, 2011. doi: 10.5772/24942.
- [22] E. Fiume, J. Barberi, E. Verné, and F. Baino, “Bioactive Glasses: From Parent 45S5 Composition to Scaffold-Assisted Tissue-Healing Therapies,” *Journal of Functional Biomaterials*, vol. 9, no. 1. 2018. doi: 10.3390/jfb9010024.

- [23] D. J. Hulsen, N. A. van Gestel, J. A. P. Geurts, and J. J. Arts, “4 - S53P4 bioactive glass,” J. J. C. Arts and J. B. T.-M. of P. J. I. (PJIs) Geurts, Eds. Woodhead Publishing, 2017, pp. 69–80. doi: <https://doi.org/10.1016/B978-0-08-100205-6.00004-5>.
- [24] A. Moghanian, M. Zohourfazeli, and M. H. M. Tajer, “The effect of zirconium content on in vitro bioactivity, biological behavior and antibacterial activity of sol-gel derived 58S bioactive glass,” *J. Non. Cryst. Solids*, vol. 546, p. 120262, 2020, doi: <https://doi.org/10.1016/j.jnoncrysol.2020.120262>.
- [25] S. Midha, T. B. Kim, W. van den Bergh, P. D. Lee, J. R. Jones, and C. A. Mitchell, “Preconditioned 70S30C bioactive glass foams promote osteogenesis in vivo,” *Acta Biomater.*, vol. 9, no. 11, pp. 9169–9182, 2013, doi: <https://doi.org/10.1016/j.actbio.2013.07.014>.
- [26] Q. Fu, M. N. Rahaman, B. Sonny Bal, R. F. Brown, and D. E. Day, “Mechanical and in vitro performance of 13–93 bioactive glass scaffolds prepared by a polymer foam replication technique,” *Acta Biomater.*, vol. 4, no. 6, pp. 1854–1864, 2008, doi: <https://doi.org/10.1016/j.actbio.2008.04.019>.
- [27] T.-H. Kim, R. Singh, K. Min Sil, J.-H. Kim, and H.-W. Kim, “Gene delivery nanocarriers of bioactive glass with unique potential to load BMP2 plasmid DNA and to internalize into mesenchymal stem cells for osteogenesis and bone regeneration,” *Nanoscale*, vol. 8, Mar. 2016, doi: [10.1039/C5NR07933K](https://doi.org/10.1039/C5NR07933K).
- [28] S. Greasley *et al.*, “Controlling particle size in the Stöber process and incorporation of calcium,” *J. Colloid Interface Sci.*, vol. 469, Feb. 2016, doi: [10.1016/j.jcis.2016.01.065](https://doi.org/10.1016/j.jcis.2016.01.065).
- [29] E. Corradini, P. S. Curti, A. B. Meniqueti, A. F. Martins, A. F. Rubira, and E.

- C. Muniz, “Recent advances in food-packing, pharmaceutical and biomedical applications of zein and zein-based materials.,” *Int. J. Mol. Sci.*, vol. 15, no. 12, pp. 22438–22470, Dec. 2014, doi: 10.3390/ijms151222438.
- [30] N. Sato, M. Kawachi, K. Noto, N. Yoshimoto, and M. Yoshizawa, “Effect of particle size reduction on crack formation in electrophoretically deposited YBCO films,” *Phys. C Supercond.*, vol. 357–360, pp. 1019–1022, 2001, doi: [https://doi.org/10.1016/S0921-4534\(01\)00510-X](https://doi.org/10.1016/S0921-4534(01)00510-X).
- [31] J. G. P. Binner, “ADVANCED CERAMIC PROCESSING AND TECHNOLOGY Volume 1”.
- [32] L. Besra and M. Liu, “A review on fundamentals and applications of electrophoretic deposition (EPD),” *Prog. Mater. Sci.*, vol. 52, no. 1, pp. 1–61, 2007, doi: 10.1016/j.pmatsci.2006.07.001.
- [33] I. Zhitomirsky, “Cathodic electrodeposition of ceramic and organoceramic materials. Fundamental aspects,” *Adv. Colloid Interface Sci.*, vol. 97, no. 1, pp. 279–317, 2002, doi: [https://doi.org/10.1016/S0001-8686\(01\)00068-9](https://doi.org/10.1016/S0001-8686(01)00068-9).
- [34] R. W. Powers, “The Electrophoretic Forming of Beta-Alumina Ceramic,” *J. Electrochem. Soc.*, vol. 122, no. 4, pp. 490–500, 1975, doi: 10.1149/1.2134246.
- [35] H. Negishi, H. Yanagishita, and H. Yokokawa, “SOLID OXIDE FUEL CELL MATERIAL POWDERS,” in *Electrophoretic Deposition, Fundamentals and Applications: Proceedings of the International Symposium*, 2002, vol. 2002, p. 214.
- [36] B. Ferrari and R. Moreno, “The conductivity of aqueous Al₂O₃ slips for electrophoretic deposition,” *Mater. Lett.*, vol. 28, no. 4, pp. 353–355, 1996, doi:

[https://doi.org/10.1016/0167-577X\(96\)00075-4](https://doi.org/10.1016/0167-577X(96)00075-4).

- [37] B. Ferrari and R. Moreno, “Electrophoretic deposition of aqueous alumina slips,” *J. Eur. Ceram. Soc.*, vol. 17, no. 4, pp. 549–556, 1997, doi: 10.1016/S0955-2219(96)00113-6.
- [38] B. a Krueger HG, Knotte A, Schindler U, Kern H, “Composite ceramic metal coatings by means of combined electrophoretic deposition,” *Mater Sci*, vol. 9, pp. 39:839–44, 2004.
- [39] M. Zarbov, I. Schuster, and L. Gal-Or, “Methodology for selection of charging agents for electrophoretic deposition of ceramic particles,” *J. Mater. Sci.*, vol. 39, no. 3, pp. 813–817, 2004, doi: 10.1023/B:JMSC.0000012908.18329.93.
- [40] P. Sarkar and P. S. Nicholson, “Electrophoretic deposition (EPD): Mechanisms, kinetics, and application to ceramics,” *Journal of the American Ceramic Society*, vol. 79, no. 8. pp. 1987–2002, 1996. doi: 10.1111/j.1151-2916.1996.tb08929.x.
- [41] F. Chen and M. Liu, “Preparation of yttria-stabilized zirconia (YSZ) films on La_{0.85}Sr_{0.15}MnO₃ (LSM) and LSM–YSZ substrates using an electrophoretic deposition (EPD) process,” *J. Eur. Ceram. Soc.*, vol. 21, no. 2, pp. 127–134, 2001, doi: [https://doi.org/10.1016/S0955-2219\(00\)00195-3](https://doi.org/10.1016/S0955-2219(00)00195-3).
- [42] R. N. Basu, C. A. Randall, and M. J. Mayo, “Fabrication of Dense Zirconia Electrolyte Films for Tubular Solid Oxide Fuel Cells by Electrophoretic Deposition,” *J. Am. Ceram. Soc.*, vol. 84, no. 1, pp. 33–40, 2001, doi: 10.1111/j.1151-2916.2001.tb00604.x.
- [43] I. Zhitomirsky and L. Gal-Or, “Electrophoretic deposition of hydroxyapatite,”

- J. Mater. Sci. Mater. Med.*, vol. 8, no. 4, pp. 213–219, 1997, doi:
10.1023/A:1018587623231.
- [44] L. Vandeperre, O. Van Der Biest, and W. J. Clegg, “Silicon carbide laminates with carbon interlayers by electrophoretic deposition,” *Key Eng. Mater.*, vol. 127–131, pp. 567–574, 1997, doi: 10.4028/www.scientific.net/kem.127-131.567.
- [45] J. Antony, “Taguchi or classical design of experiments: A perspective from a practitioner,” *Sens. Rev.*, vol. 26, no. 3, pp. 227–230, 2006, doi: 10.1108/02602280610675519.
- [46] R. K. Roy, *Design of experiments using the Taguchi approach: 16 steps to product and process improvement*. John Wiley & Sons, 2001.
- [47] J. M. Macak and P. Schmuki, “Anodic growth of self-organized anodic TiO₂ nanotubes in viscous electrolytes,” *Electrochim. Acta*, vol. 52, no. 3, pp. 1258–1264, 2006, doi: 10.1016/j.electacta.2006.07.021.
- [48] J. M. Macak *et al.*, “TiO₂ nanotubes: Self-organized electrochemical formation, properties and applications,” *Curr. Opin. Solid State Mater. Sci.*, vol. 11, no. 1–2, pp. 3–18, 2007, doi: 10.1016/j.cossms.2007.08.004.
- [49] R. Bott, “Synthesis and Characterization of Titania Nanotubes for Photocatalytic Water- Splitting and Carbon Dioxide Methanation,” *Igarss 2014*, no. 1, pp. 1–5, 2014.
- [50] S. A. Batool, K. Ahmad, M. Irfan, M. Atiq, and U. Rehman, “Zn – Mn-Doped Mesoporous Bioactive Glass Nanoparticle-Loaded Zein Coatings for Bioactive and Antibacterial Orthopedic Implants,” 2022.

- [51] W. Li and D. Zhao, "Extension of the stöber method to construct mesoporous SiO₂ and TiO₂ shells for uniform multifunctional core-shell structures," *Adv. Mater.*, vol. 25, no. 1, pp. 142–149, 2013, doi: 10.1002/adma.201203547.
- [52] S. Bano *et al.*, "Synthesis and characterization of silver-strontium (Ag-Sr)-doped mesoporous bioactive glass nanoparticles," *Gels*, vol. 7, no. 2, pp. 1–15, 2021, doi: 10.3390/gels7020034.
- [53] L. V. Taveira, J. M. Macák, H. Tsuchiya, L. F. P. Dick, and P. Schmuki, "Initiation and Growth of Self-Organized TiO₂ Nanotubes Anodically Formed in NH₄F/(NH₄)₂SO₄ Electrolytes," *J. Electrochem. Soc.*, vol. 152, no. 10, p. B405, 2005, doi: 10.1149/1.2008980.
- [54] S. P. Albu *et al.*, "Formation of double-walled TiO₂ nanotubes and robust anatase membranes," *Adv. Mater.*, vol. 20, no. 21, pp. 4135–4139, 2008.
- [55] E. Panaitescu, "Titanium oxide nanotubes: Synthesis, properties and applications for solar energy harvesting," no. April, p. 30, 2009, [Online]. Available: http://adsabs.harvard.edu/cgi-bin/nph-data_query?bibcode=2009PhDT.....30P&link_type=EJOURNAL%0Apapers3://publication/uuid/40B2C623-AC67-4A7C-AB7E-15AFD5E5E727
- [56] C. Yao and T. J. Webster, "Anodization: A promising nano-modification technique of titanium implants for orthopedic applications," *J. Nanosci. Nanotechnol.*, vol. 6, no. 9–10, pp. 2682–2692, 2006, doi: 10.1166/jnn.2006.447.
- [57] K. E. Tanner, *Titanium in Medicine*, vol. 216, no. 3. 2002. doi: 10.1243/0954411021536432.

- [58] B. Yang, C. K. Ng, M. K. Fung, C. C. Ling, A. B. Djurišić, and S. Fung, “Annealing study of titanium oxide nanotube arrays,” *Mater. Chem. Phys.*, vol. 130, no. 3, pp. 1227–1231, 2011, doi: 10.1016/j.matchemphys.2011.08.063.
- [59] L. R. Rivera, J. Dippel, and A. R. Boccaccini, “Formation of Zein/Bioactive Glass Layers Using Electrophoretic Deposition Technique,” *{ECS} Trans.*, vol. 82, no. 1, pp. 73–80, Jan. 2018, doi: 10.1149/08201.0073ecst.
- [60] J. P. Rao and K. E. Geckeler, “Polymer nanoparticles: Preparation techniques and size-control parameters,” *Prog. Polym. Sci.*, vol. 36, no. 7, pp. 887–913, 2011, doi: 10.1016/j.progpolymsci.2011.01.001.
- [61] H. Chen and Q. Zhong, “A novel method of preparing stable zein nanoparticle dispersions for encapsulation of peppermint oil,” *Food Hydrocoll.*, vol. 43, pp. 593e602-602, 2015, doi: 10.1016/j.foodhyd.2014.07.018.
- [62] A. Pawlik, M. A. U. Rehman, Q. Nawaz, F. E. Bastan, G. D. Sulka, and A. R. Boccaccini, “Fabrication and characterization of electrophoretically deposited chitosan-hydroxyapatite composite coatings on anodic titanium dioxide layers,” *Electrochim. Acta*, vol. 307, pp. 465–473, 2019, doi: 10.1016/j.electacta.2019.03.195.
- [63] J. Hum, S. Naseri, and A. R. Boccaccini, “Bioactive glass combined with zein as composite material for the application in bone tissue engineering,” vol. 4, no. 1, pp. 72–81, 2018, doi: doi:10.1515/bglass-2018-0007.
- [64] T. M. Costelloe, “Kant’s Conception of Moral Character: The ‘Critical’ Link of Morality, Anthropology, and Reflective Judgment (review),” *J. Hist. Philos.*, vol. 39, no. 3, pp. 445–446, 2001, doi: 10.1353/hph.2003.0120.

- [65] A. Standard, “Standard Test Method for Film Hardness by Pencil Test,” *D3363–20*, pp. 3320–3363, 2020.
- [66] A. ASTM, “D3359-17 Standard Test Methods for Rating Adhesion by Tape Test,” *West Conshohocken, PA ASTM Int.*, 2017.
- [67] T. Kokubo and H. Takadama, “How useful is SBF in predicting in vivo bone bioactivity?,” *Biomaterials*, vol. 27, no. 15, pp. 2907–2915, 2006, doi: 10.1016/j.biomaterials.2006.01.017.